

# Strangeness production in $pp$ and $p\text{Pb}$ collisions

Clara Landesa Gómez  
on behalf of the LHCb collaboration



**IGFAE**  
Instituto Galego de Física de Altas Energías



**XUNTA DE GALICIA**



Cofinanciado por  
la Unión Europea

 Fondos Europeos

# Outline

1. The LHCb experiment. Data samples.
2. Heavy strange hadrons in small systems.
3. Recent LHCb results.

Measuring system size. Multiplicity proxies.

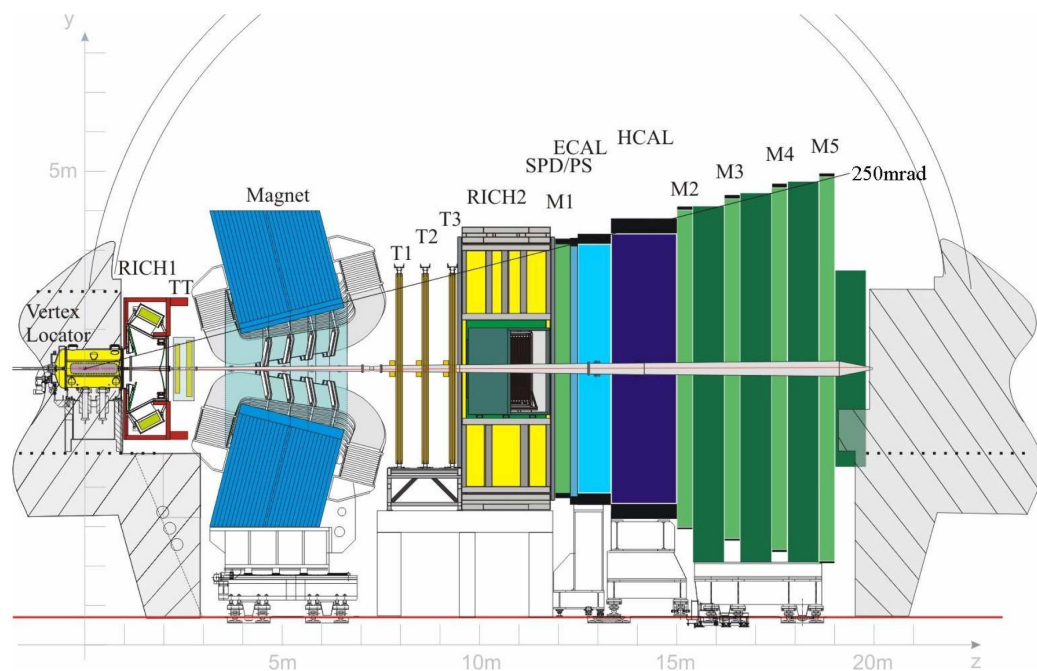
- $B_s^0/B^0$  ratio with multiplicity in  $pp$  collisions at 13 TeV ..... [Phys. Rev. Lett. 131 \(2023\) 061901](#)
- $D_s^+/D^{+0}$  ratio in  $pPb$  collisions at 5 TeV ..... [JHEP 01 \(2024\) 070](#)
- $D_s^+/D^+$  ratio in  $pPb$  collisions at 8 TeV ..... [arXiv:2311.08490 NEW!](#)
- $\Xi_c^+/\Lambda_c^+$  ratio in  $pPb$  at 8 TeV ..... [Phys. Rev. C 109 \(2024\) 044901](#)

4. Conclusion and prospects.

# The LHCb experiment.

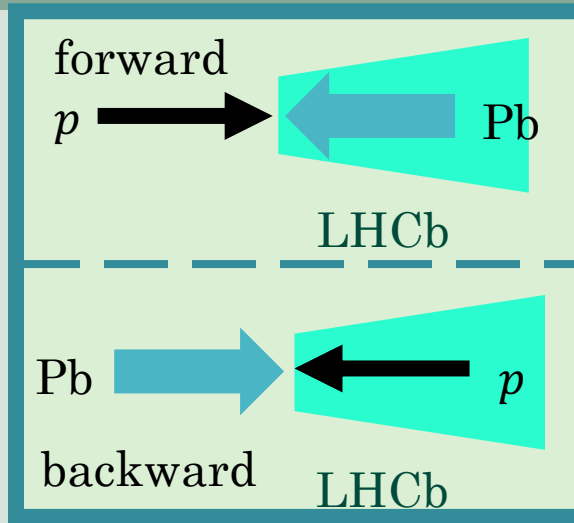
- From heavy flavour physics to general-purpose detector in the forward region.
- Fully instrumented forward detector  $2 < \eta < 5$ .
- Excellent tracking, momentum resolution and particle identification.

[JINST 3 \(2008\) S08005](#)

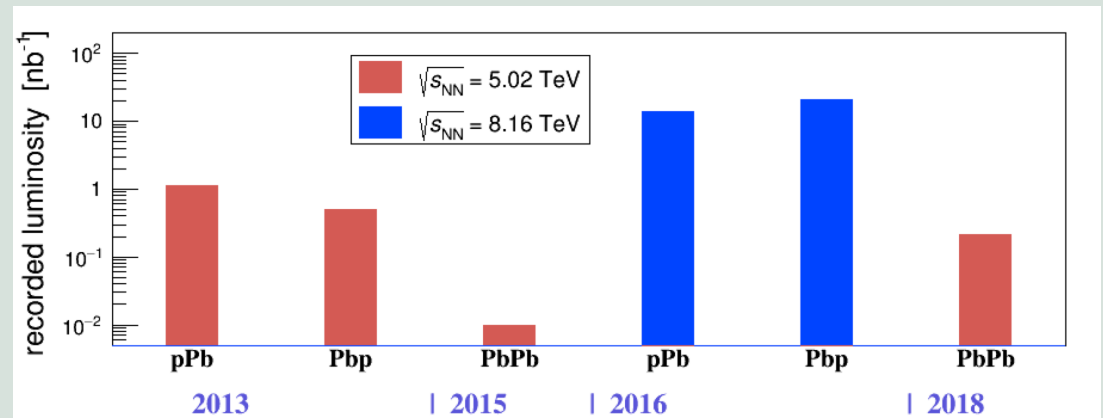


# Data samples.

- The results in this presentation are from *small collision systems*.
- $pp$  collisions  $\sqrt{s} = 13 \text{ TeV}$ ,  $\int \mathcal{L} dt = 5.4 \text{ fb}^{-1}$
- $p\text{Pb}$  collisions at  $\sqrt{s_{NN}} = 5 \text{ TeV}$ 
  - Forward  $\int \mathcal{L} dt = 1.06 \text{ nb}^{-1}$
  - Backward  $\int \mathcal{L} dt = 0.52 \text{ nb}^{-1}$
- $p\text{Pb}$  collisions at  $\sqrt{s_{NN}} = 8 \text{ TeV}$ 
  - Forward  $\int \mathcal{L} dt = 12.18 \text{ nb}^{-1}$
  - Backward  $\int \mathcal{L} dt = 18.57 \text{ nb}^{-1}$



$$y_{\text{lab}} - y^* \approx 0.5 \times \log\left(\frac{A}{Z}\right) = 0.465$$



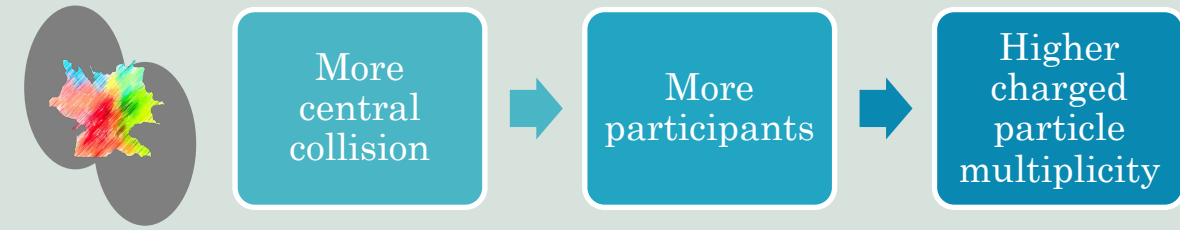
# Heavy strange hadrons in small systems.

- Why heavy strange hadrons?
  - Because of their **strangeness** content.
  - Because they offer unique probes of the **hadronization mechanism**.

# Heavy strange hadrons in small systems.

## Strangeness as a QGP signature

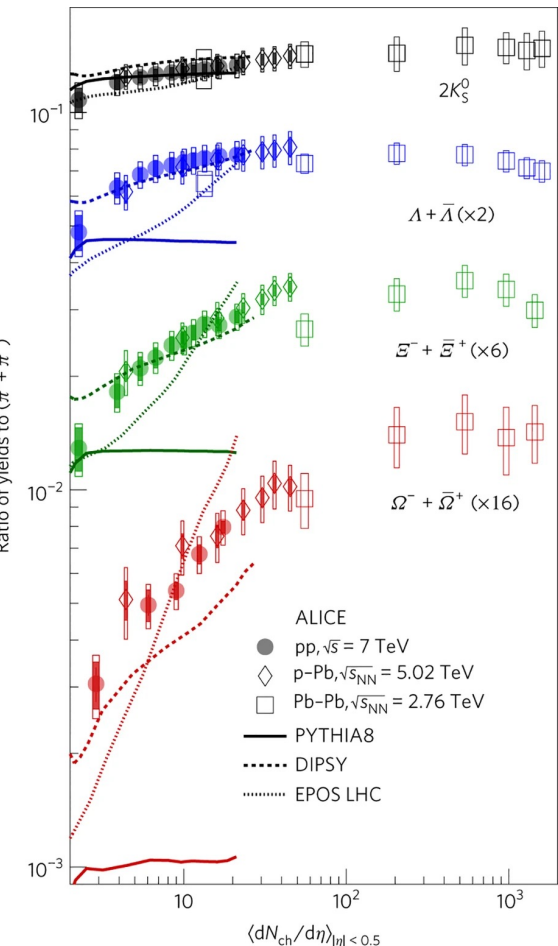
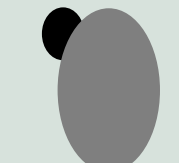
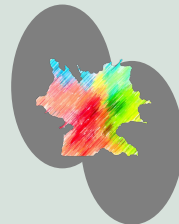
- In PbPb collisions, the enhancement of strange hadrons in high multiplicity (low centrality) events was originally postulated as a QGP signature.



# Heavy strange hadrons in small systems.

## Strangeness as a QGP signature

- In PbPb collisions, the enhancement of strange hadrons in high multiplicity (low centrality) events was originally postulated as a QGP signature.
- Recent findings show universal strangeness enhancement with the event charged particle multiplicity in *small systems*.

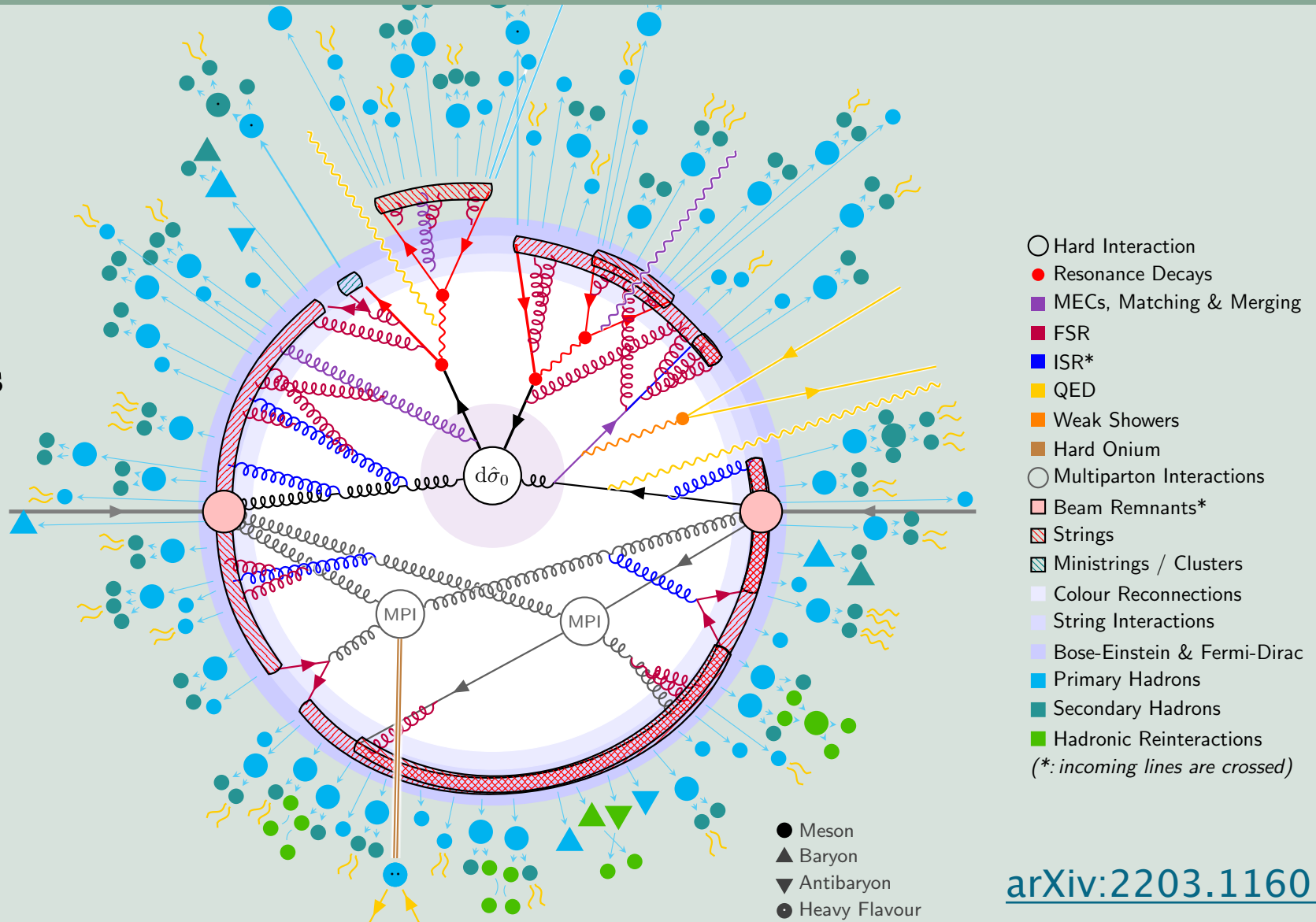


[Nature Phys 13, 535-539 \(2017\)](#)

# Heavy strange hadrons in small systems.

- The hadronization mechanism reflects the properties of the hadronic matter.

**Fragmentation:** Showers produced by outgoing partons form into hadrons.



arXiv:2203.11601

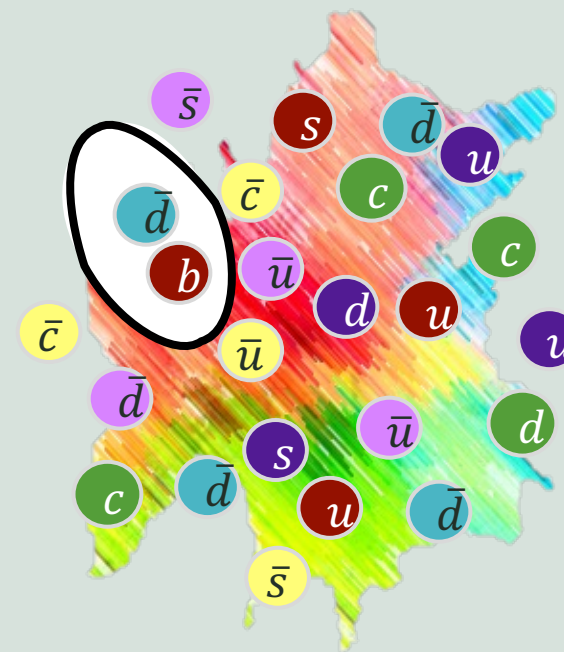
# Heavy strange hadrons in small systems.

- The hadronization mechanism

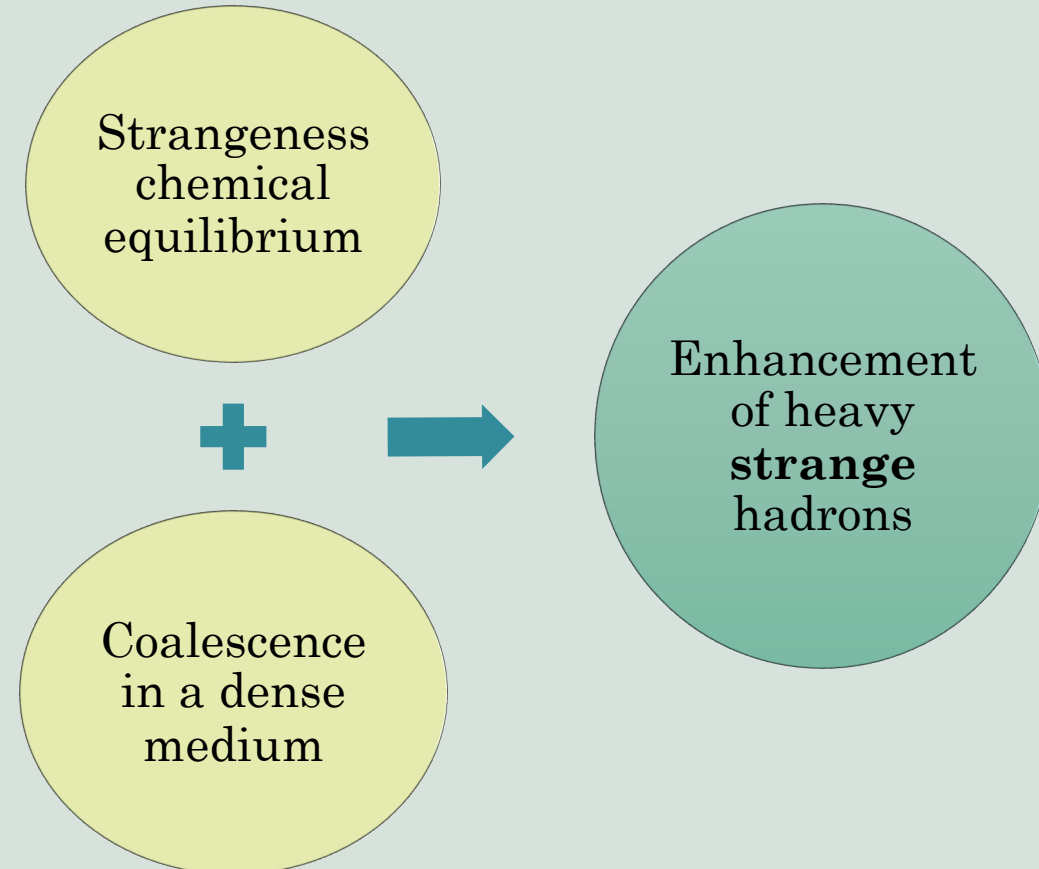
reflects the properties of the hadronic matter.

**Fragmentation:** Showers produced by outgoing partons form into hadrons.

**Coalescence:** Readily available quarks combine to form colour singlets. Requires multiple quark wavefunctions to overlap in position and velocity.



# Heavy strange hadrons in small systems.



# Recent LHCb results.

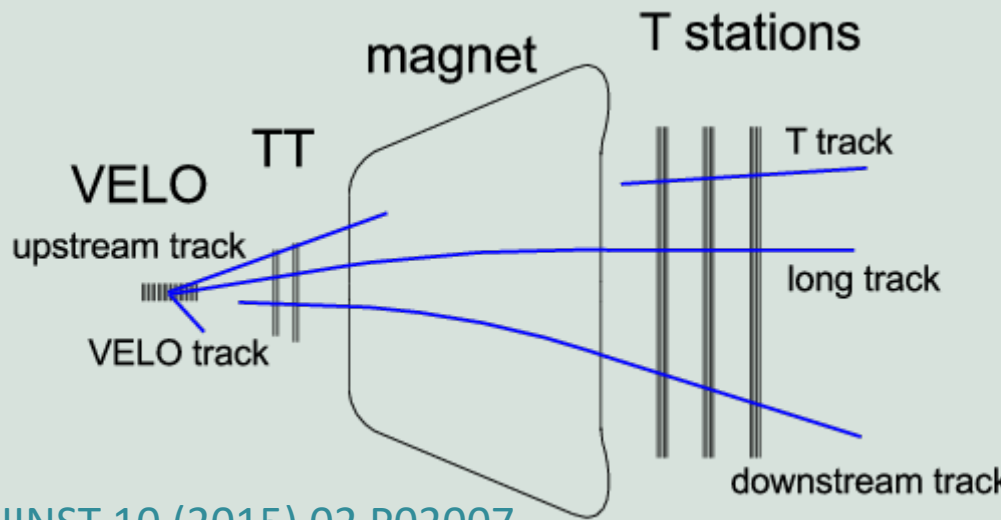
- We present recent LHCb measurements of strange hadrons in the heavy quark sector.
- We focus on the ratios of production of strange over non-strange particles, to study a potential enhancement of strange quarks.

$$R_{S/N} = \frac{\sigma_S}{\sigma_N}$$

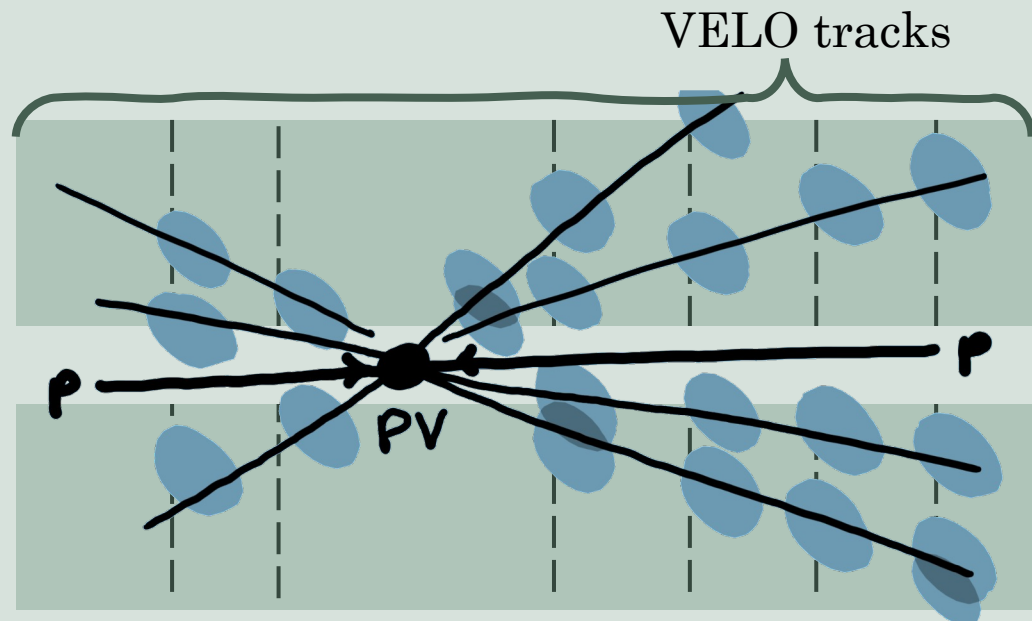
- Some results are presented as a function of the event charged particle multiplicity.

# Measuring the system size. Multiplicity proxies.

- $N_{\text{tracks}}^{\text{VELO}}$ : Total number of charged tracks reconstructed by the VELO detector.

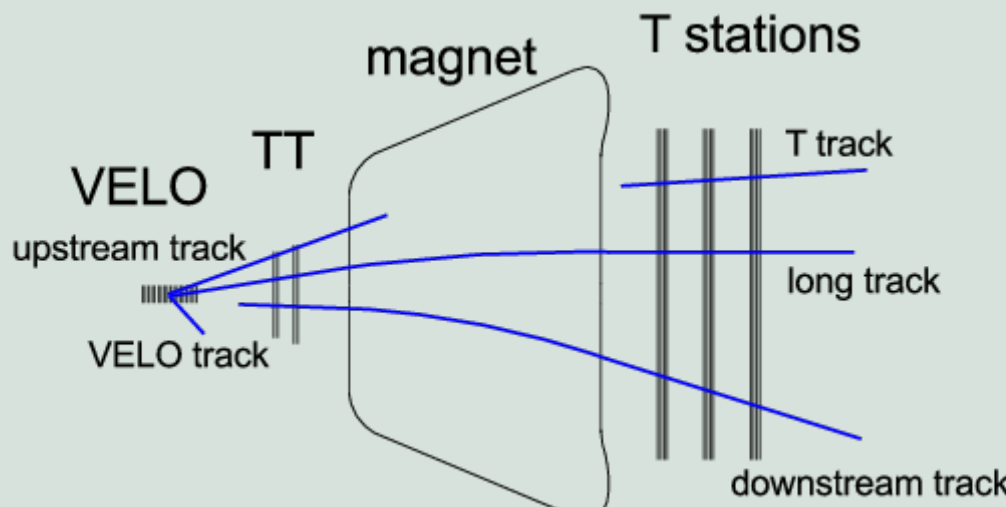


[JINST 10 \(2015\) 02 P02007](#)

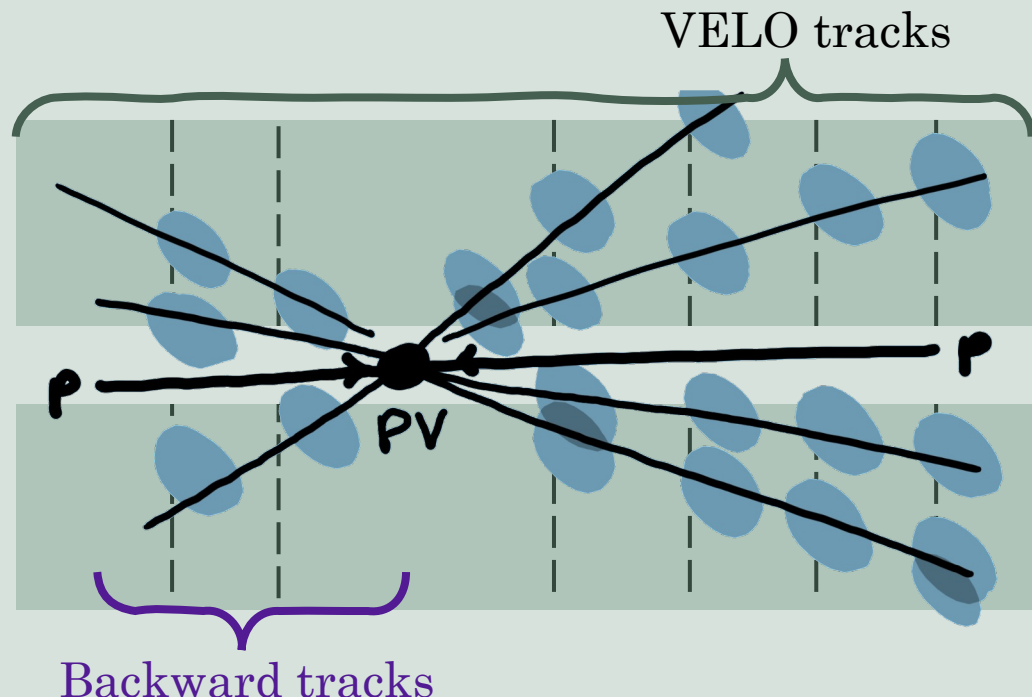


# Measuring the system size. Multiplicity proxies.

- $N_{\text{tracks}}^{\text{VELO}}$ : Total number of charged tracks reconstructed by the VELO detector.
- $N_{\text{tracks}}^{\text{back}}$ : Subset of VELO tracks that point in the backward direction, away from LHCb ( $-3.5 < \eta < -1.5$ ).

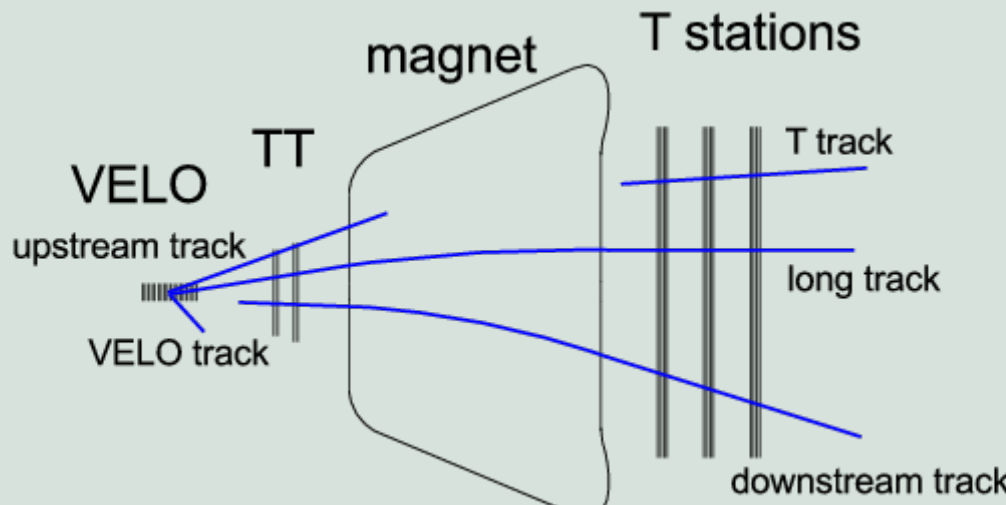


[JINST 10 \(2015\) 02 P02007](#)

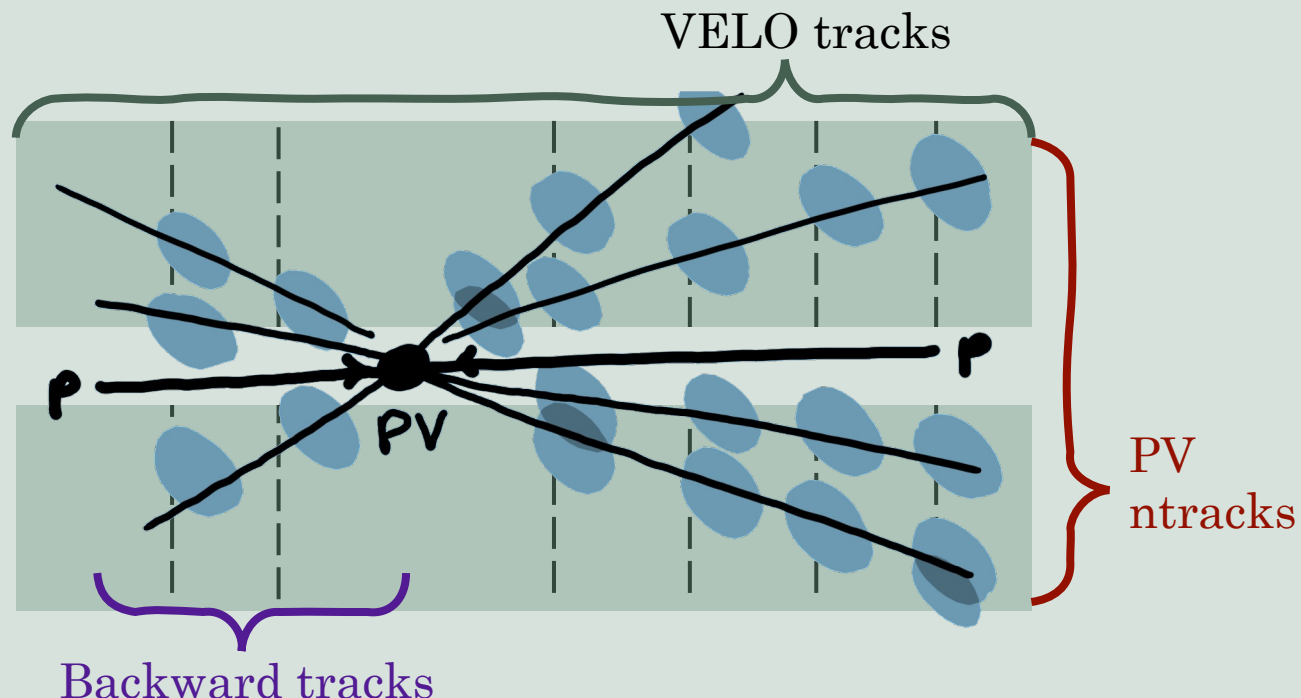


# Measuring the system size. Multiplicity proxies.

- $N_{\text{tracks}}^{\text{VELO}}$ : Total number of charged tracks reconstructed by the VELO detector.
- $N_{\text{tracks}}^{\text{back}}$ : Subset of VELO tracks that point in the backward direction, away from LHCb ( $-3.5 < \eta < -1.5$ ).
- $N_{\text{tracks}}^{\text{PV}}$ : VELO tracks used to reconstruct the primary vertex.

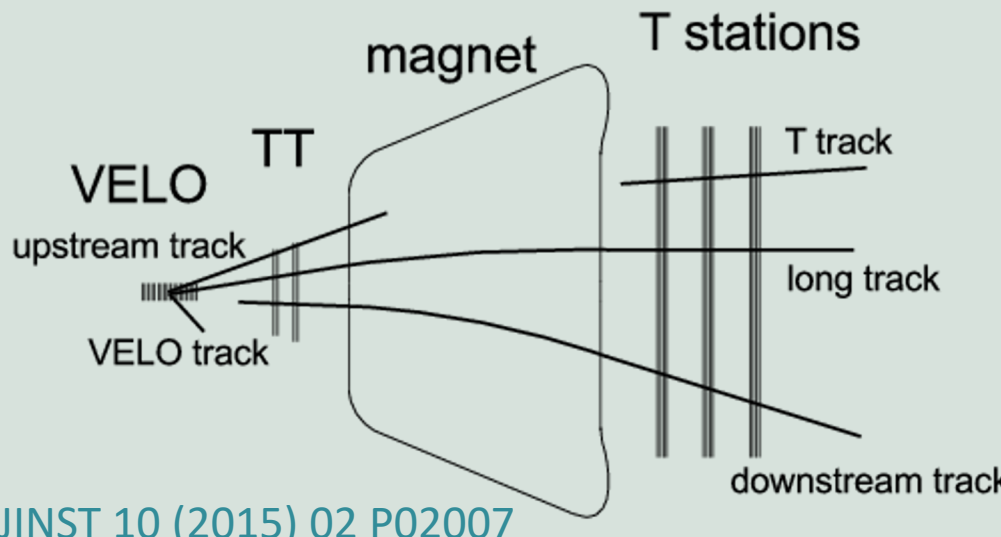


JINST 10 (2015) 02 P02007

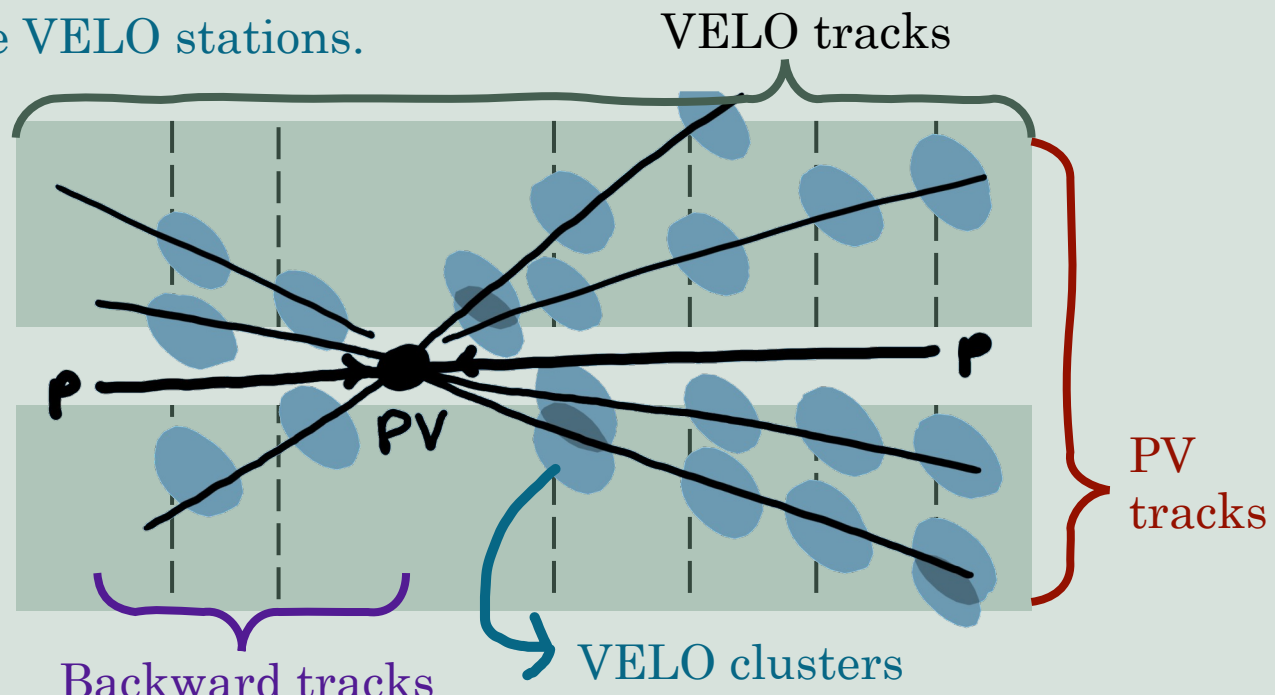


# Measuring the system size. Multiplicity proxies.

- $N_{\text{tracks}}^{\text{VELO}}$ : Total number of charged tracks reconstructed by the VELO detector.
- $N_{\text{tracks}}^{\text{back}}$ : Subset of VELO tracks that point in the backward direction, away from LHCb ( $-3.5 < \eta < -1.5$ ).
- $N_{\text{tracks}}^{\text{PV}}$ : VELO tracks used to reconstruct the primary vertex.
- $N_{\text{clusters}}^{\text{VELO}}$ : Number of energy clusters deposited in the VELO stations.



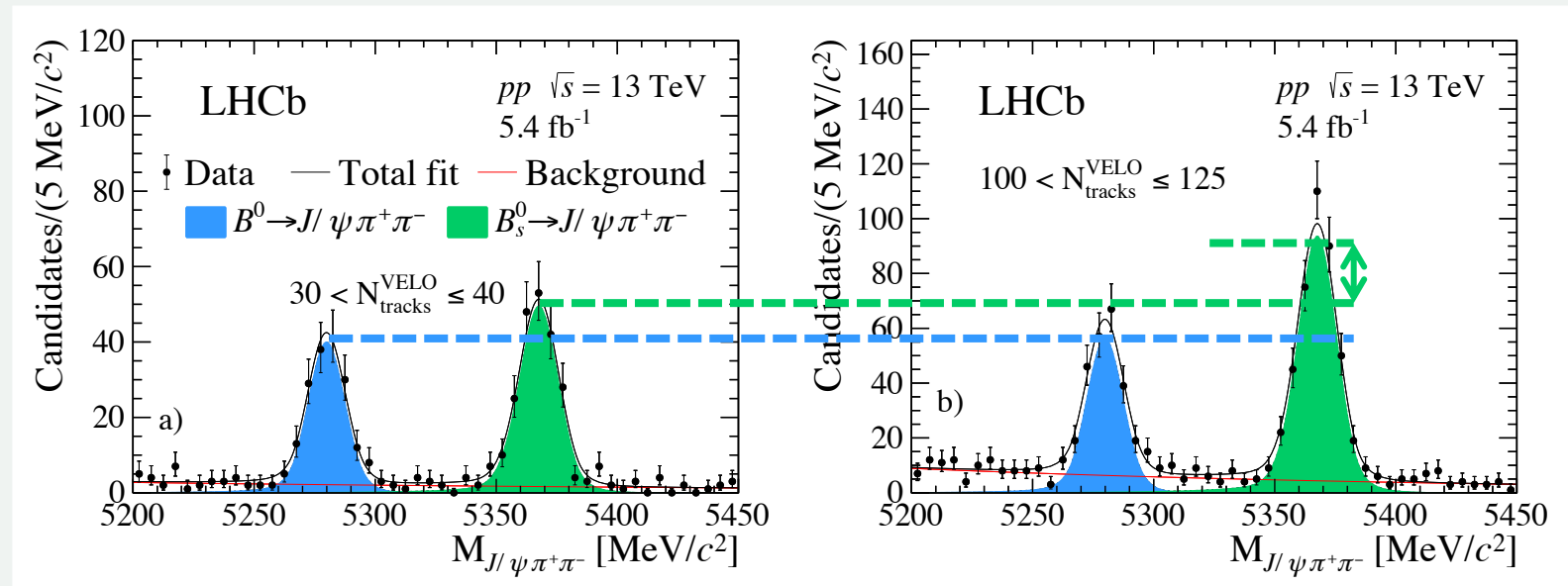
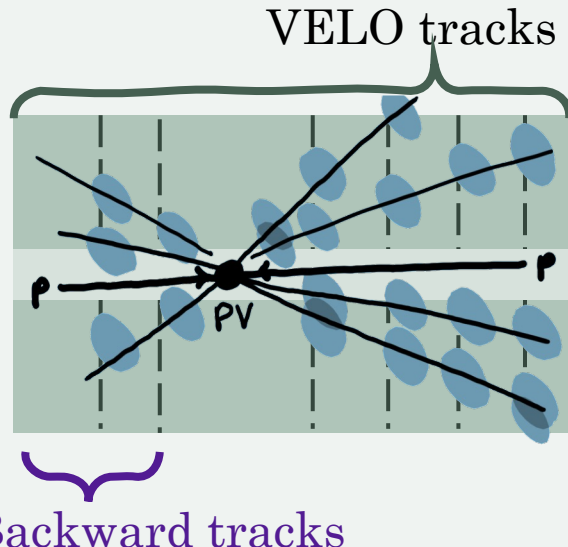
JINST 10 (2015) 02 P02007



# $B_s^0/B^0$ ratio with multiplicity $pp$ collisions at $\sqrt{s} = 13$ TeV

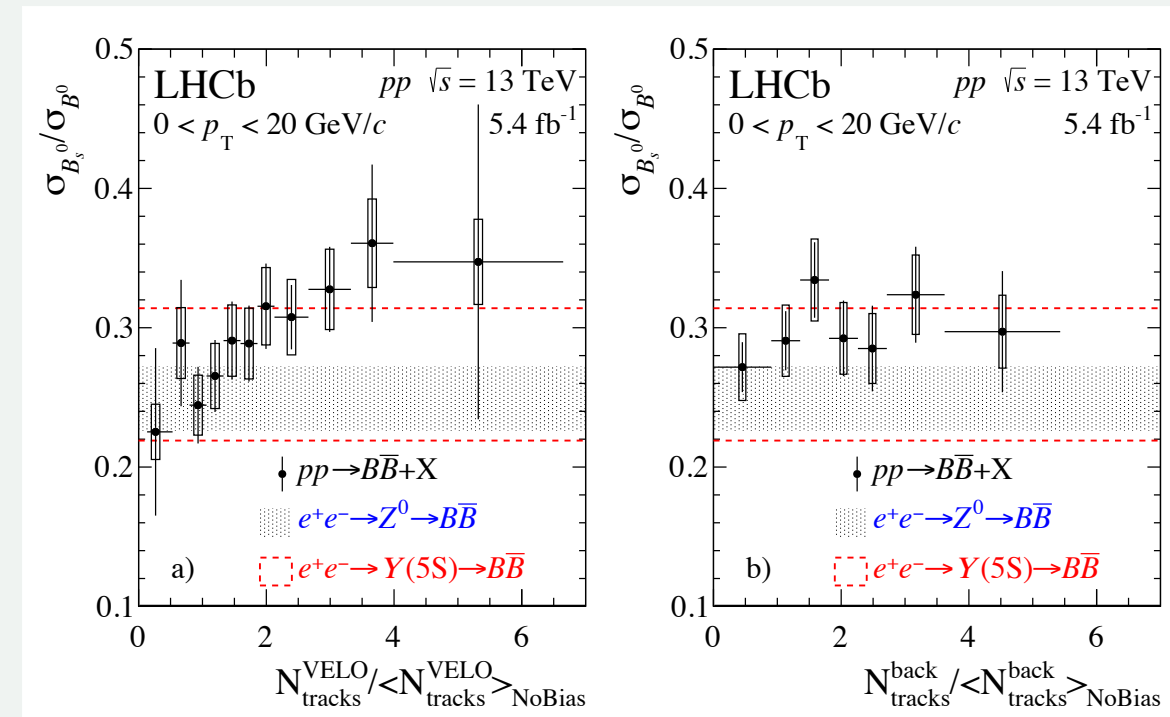


- $B_{(s)}^0 \rightarrow (J/\psi \rightarrow \mu^+\mu^-)\pi^+\pi^-$
- The multiplicity is estimated with  $N_{\text{VELO tracks}}$  and  $N_{\text{back tracks}}$ .



Apparent increase of the  $B_s^0$  yield compared to  $B^0$  with multiplicity

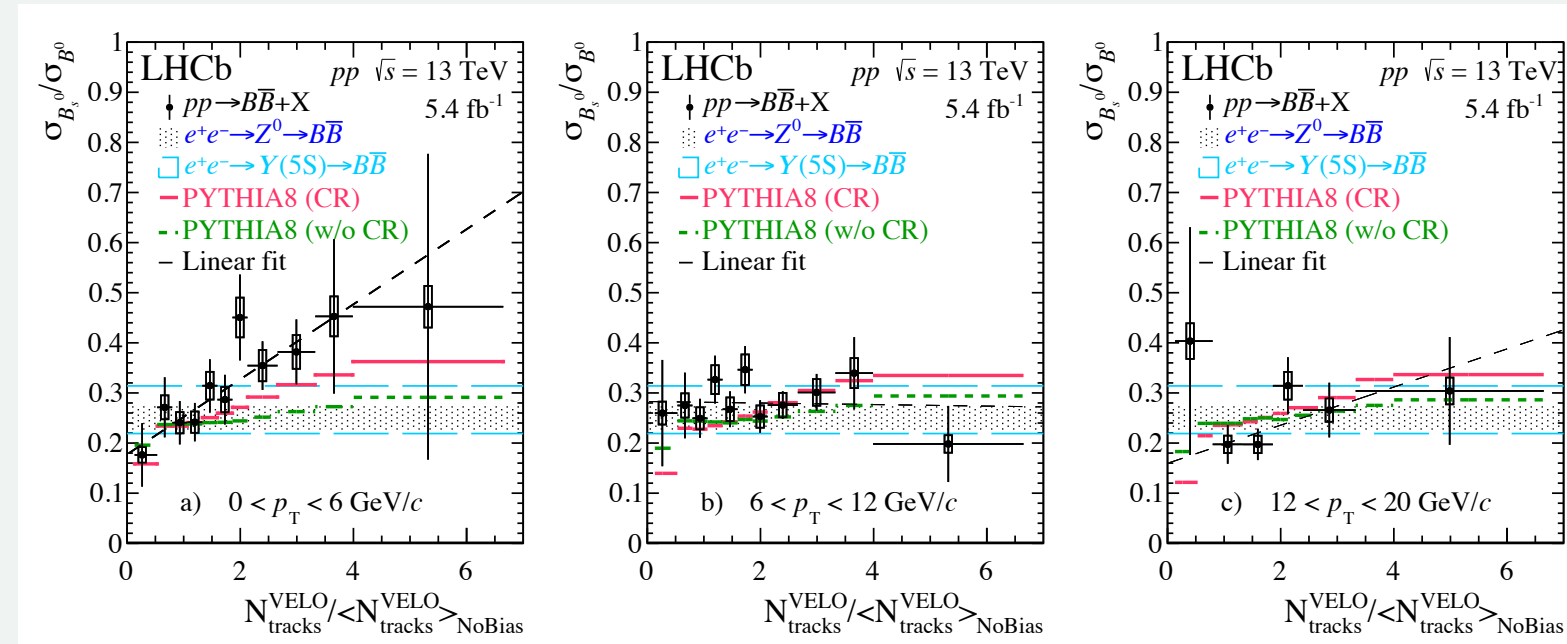
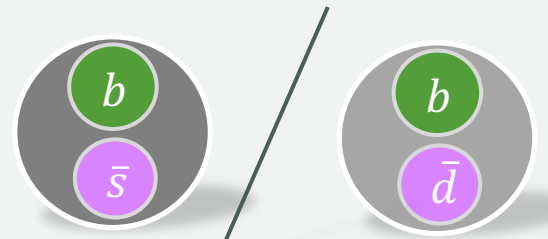
- Ratio enhancement observed with VELO tracks.
- No significant enhancement with backward tracks. This hints that the mechanism responsible for the increase in the ratio is related to the local particle density.
- Results coherent with  $e^+e^-$  measurements at low multiplicity.



Results quoted in normalised multiplicity

- Measurement in  $p_T$  bins.
- Ratio enhancement notable at  $p_T < 6 \text{ GeV}/c$

Qualitatively compatible with coalescence.



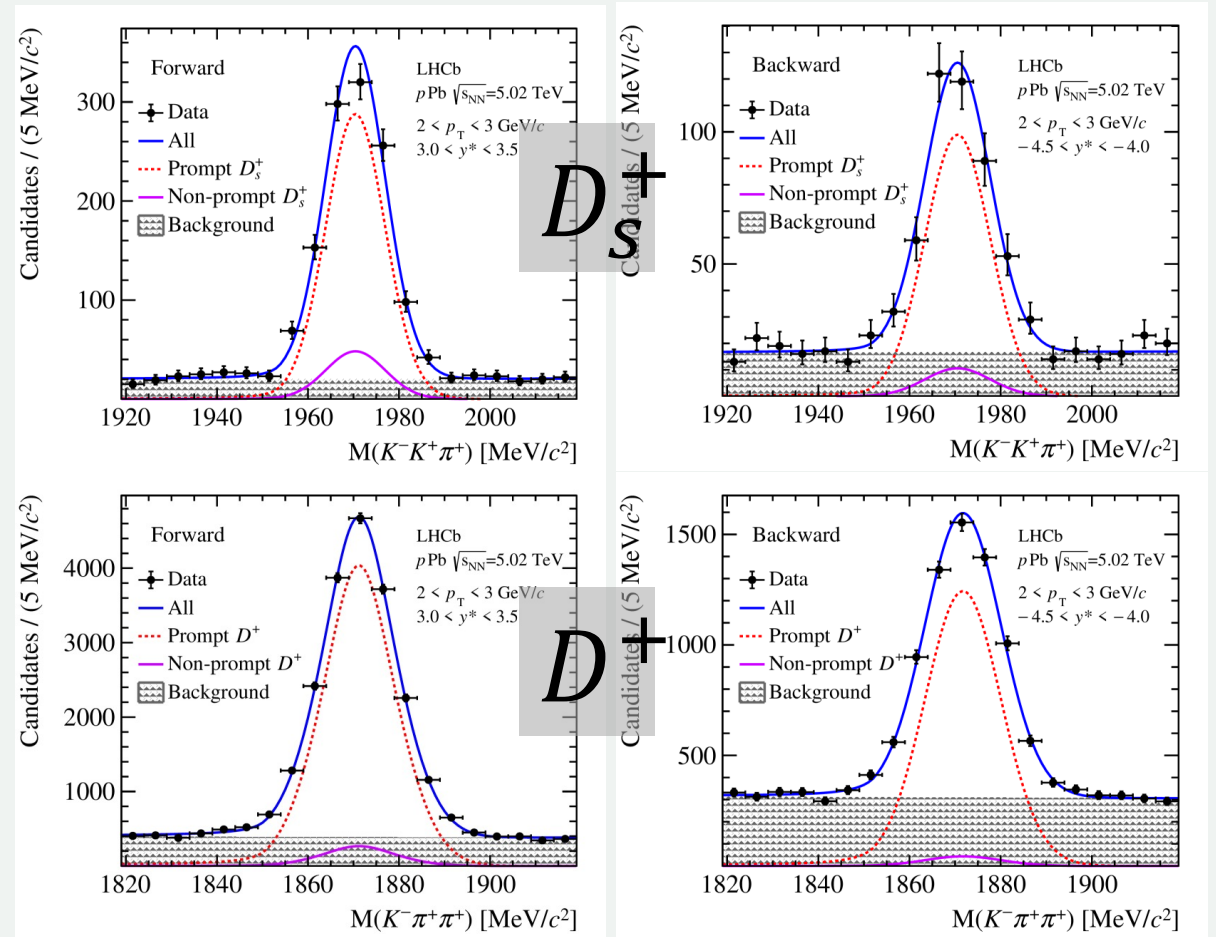
# $D_s^+/D^+$ ratio $p\text{Pb}$ collisions at $\sqrt{s_{NN}} = 5 \text{ TeV}$



$D_s^+ \rightarrow K^- K^+ \pi^+$ , BR=  $(2.24 \pm 0.15)\%$

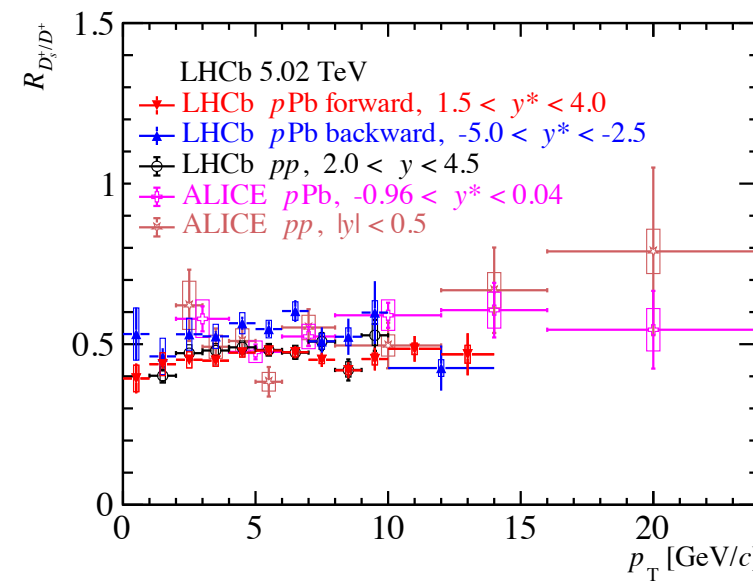
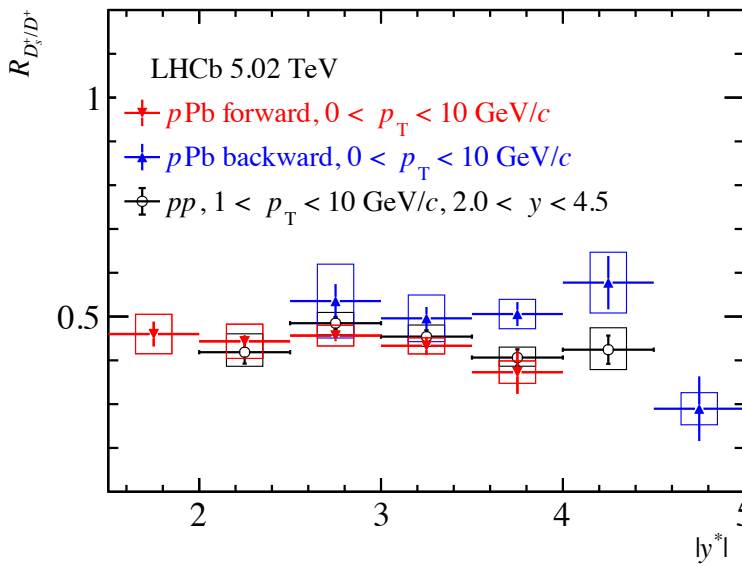
$D^+ \rightarrow K^- \pi^+ \pi^+$ , BR=  $(9.38 \pm 0.15)\%$

- The prompt contribution is selected by seeking candidates whose momentum points to the interaction vertex.

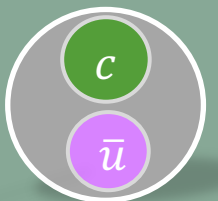
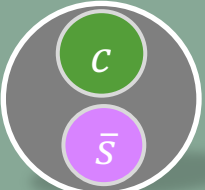




- No enhancement of the yield of strange hadrons at high transverse momentum or rapidity.
- Although not significantly, the ratio of  $D_s^+/D^+$  for backward collisions is systematically above that of forward collisions.

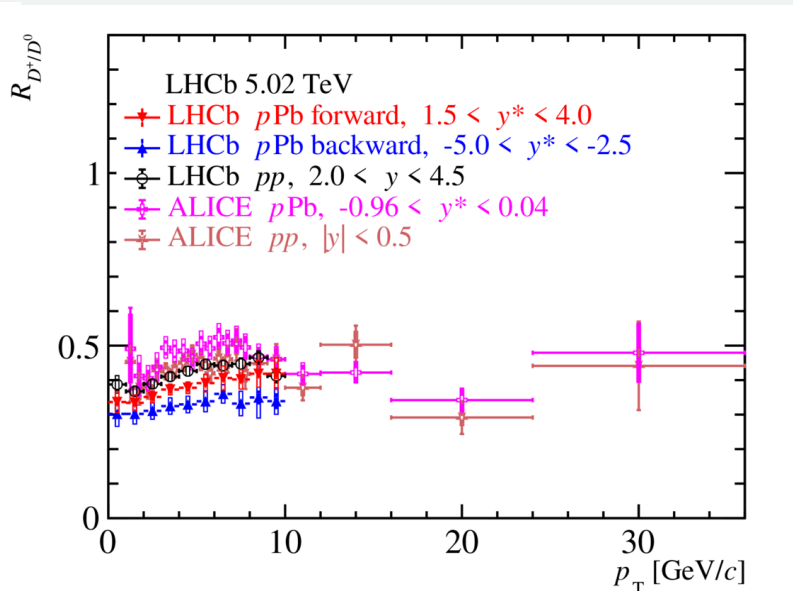
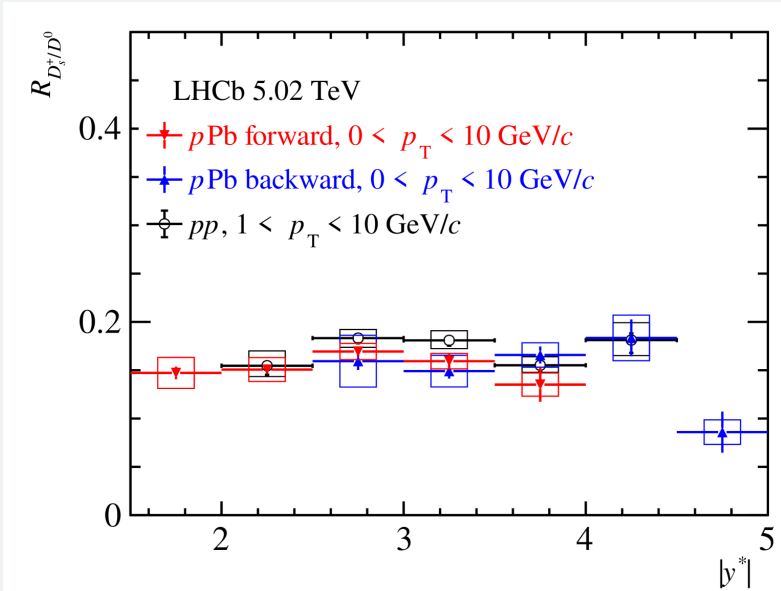


Backward collisions have on average  $\sim 1.6$  times the multiplicity of forward collisions.



# $D_s^+/D^0$ ratio $p\text{Pb}$ collisions at $\sqrt{s_{NN}} = 5 \text{ TeV}$

- No enhancement of the yield of strange hadrons at high transverse momentum or rapidity.
- In this case, the backward results are not systematically above the forward results.



Backward collisions have on average  $\sim 1.6$  times the multiplicity of forward collisions.

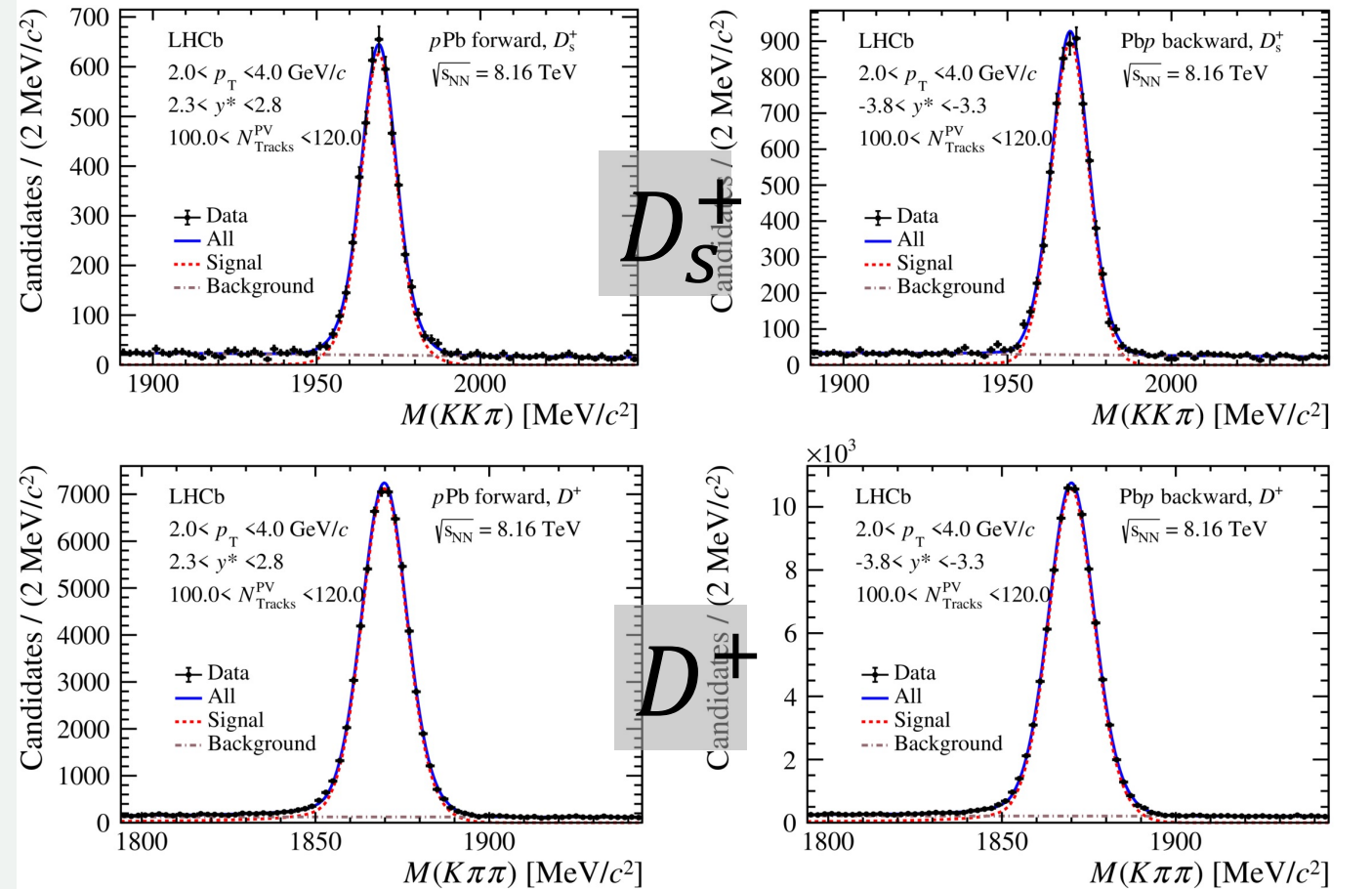
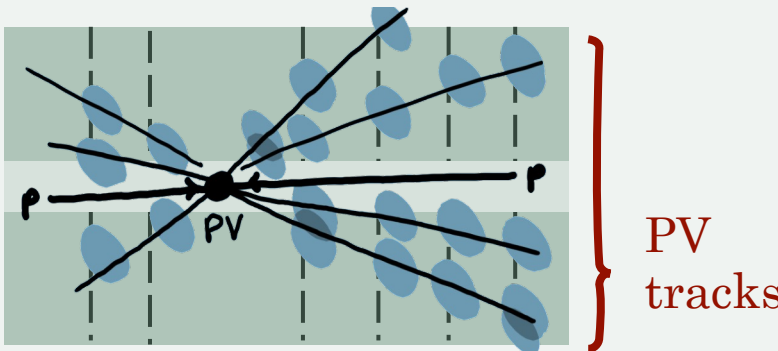
# $D_s^+/D^+$ ratio $p\text{Pb}$ collisions at $\sqrt{s_{NN}} = 8 \text{ TeV}$



$D_s^+ \rightarrow K^- K^+ \pi^+$ , BR=  $(2.24 \pm 0.15)\%$

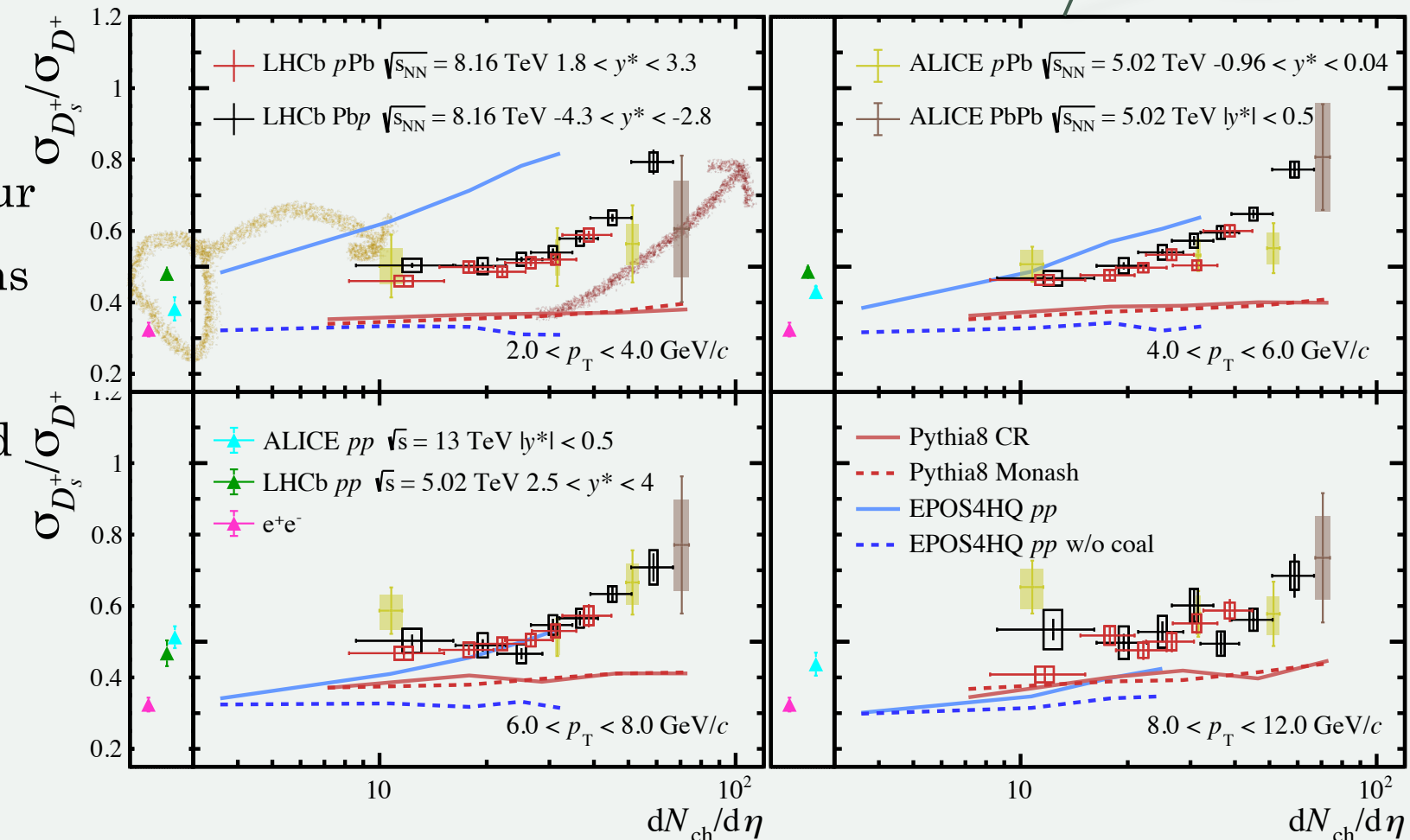
$D^+ \rightarrow K^- \pi^+ \pi^+$ , BR=  $(9.38 \pm 0.15)\%$

- The prompt contribution is selected.
- The multiplicity is estimated with  $N_{\text{tracks}}^{\text{PV}} \cdot N_{\text{ch}}$  is obtained in the forward region ( $2 < \eta < 4.8$ ) by applying corrections based on simulation.

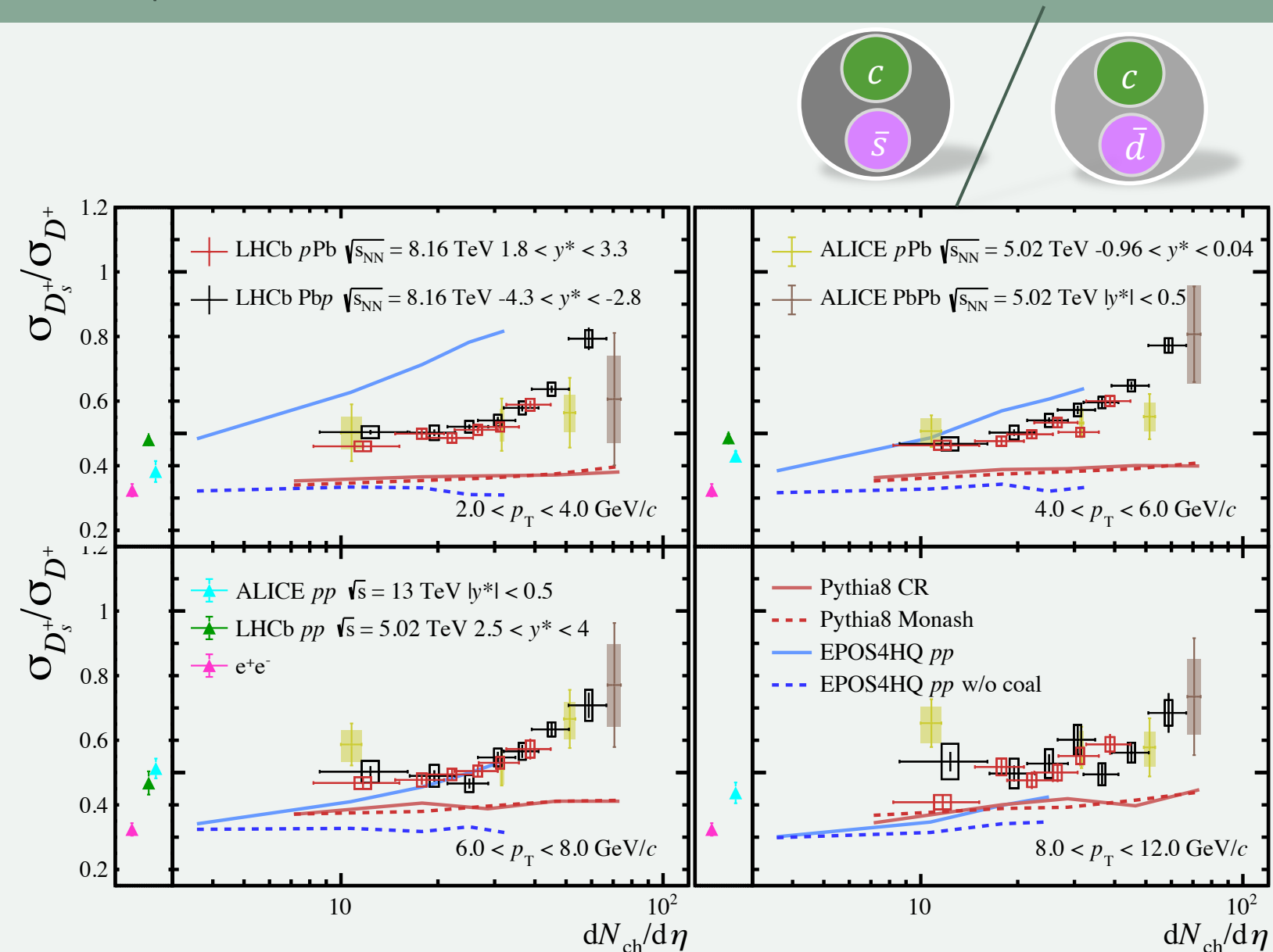


$\sigma_{D_s^+}/\sigma_{D^+}$  has an increasing trend with  $dN_{\text{ch}}/d\eta$  for all  $p_T$  intervals.

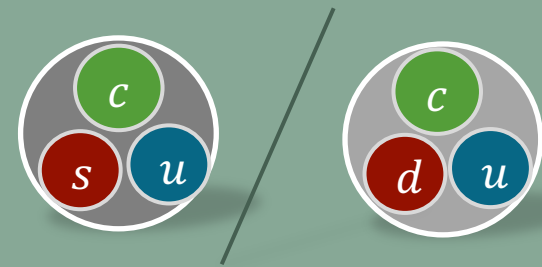
- At **low multiplicity**, the results resemble those of  $pp$  collisions.
- At **high multiplicity**, a behaviour similar to that of  $\text{PbPb}$  collisions if observed.
- The trend is similar for forward and backward rapidities.
- More enhancement at low  $p_T$ , which is qualitatively compatible with coalescence.



- All the predictions show some discrepancies with data.
- EPOS4HQ depicts the increasing trend across all  $p_T$  intervals when accounting for a coalescence hadronization mechanism.



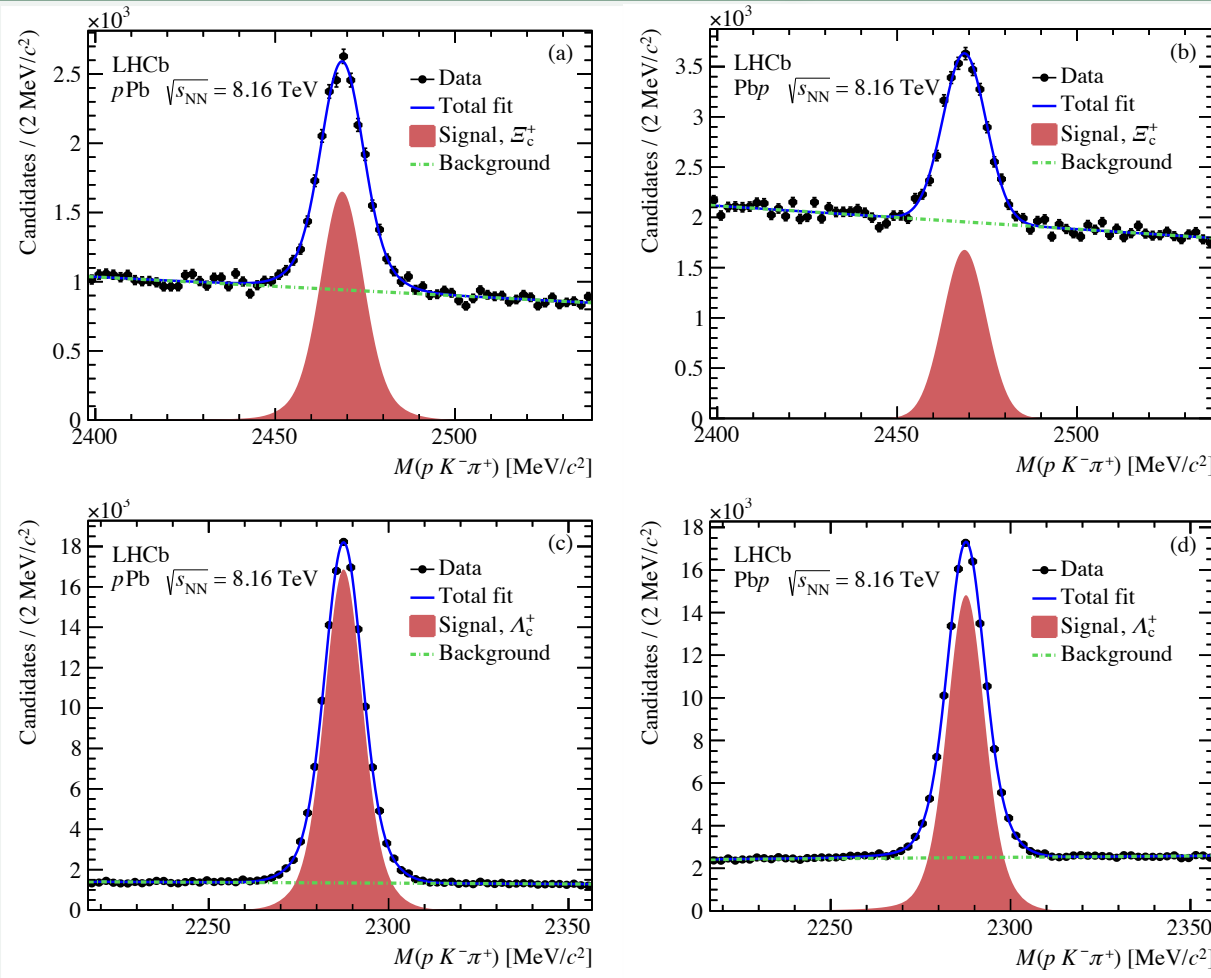
# $\Xi_c^+/\Lambda_c^+$ ratio $p\text{Pb}$ collisions at $\sqrt{s_{NN}} = 8 \text{ TeV}$



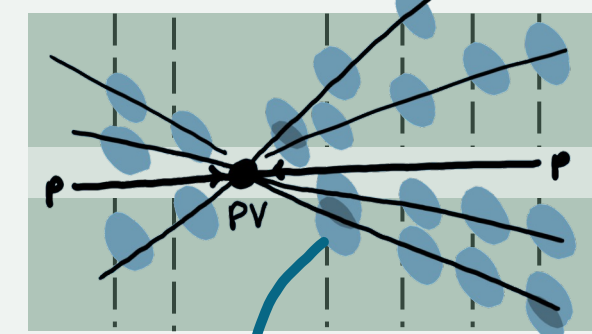
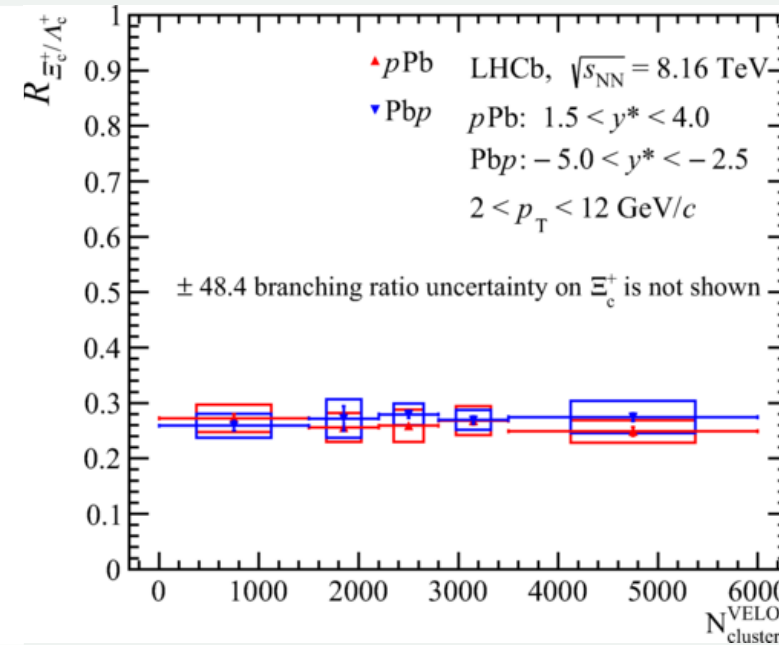
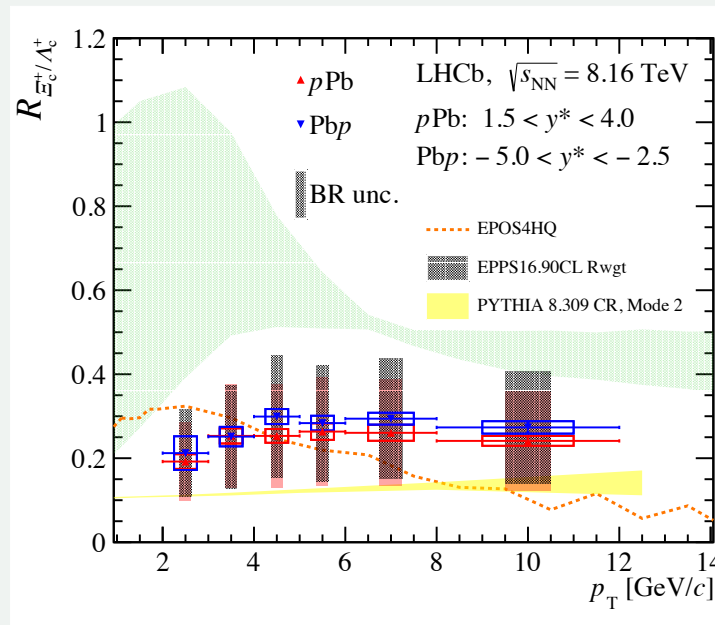
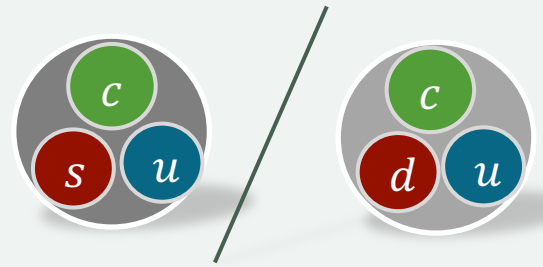
$\Xi_c^+ \rightarrow p^+ K^- \pi^+$ , BR =  $(0.62 \pm 0.30)\%$

$\Lambda_c^+ \rightarrow p^+ K^- \pi^+$ , BR =  $(6.28 \pm 0.32)\%$

The prompt contribution is selected.



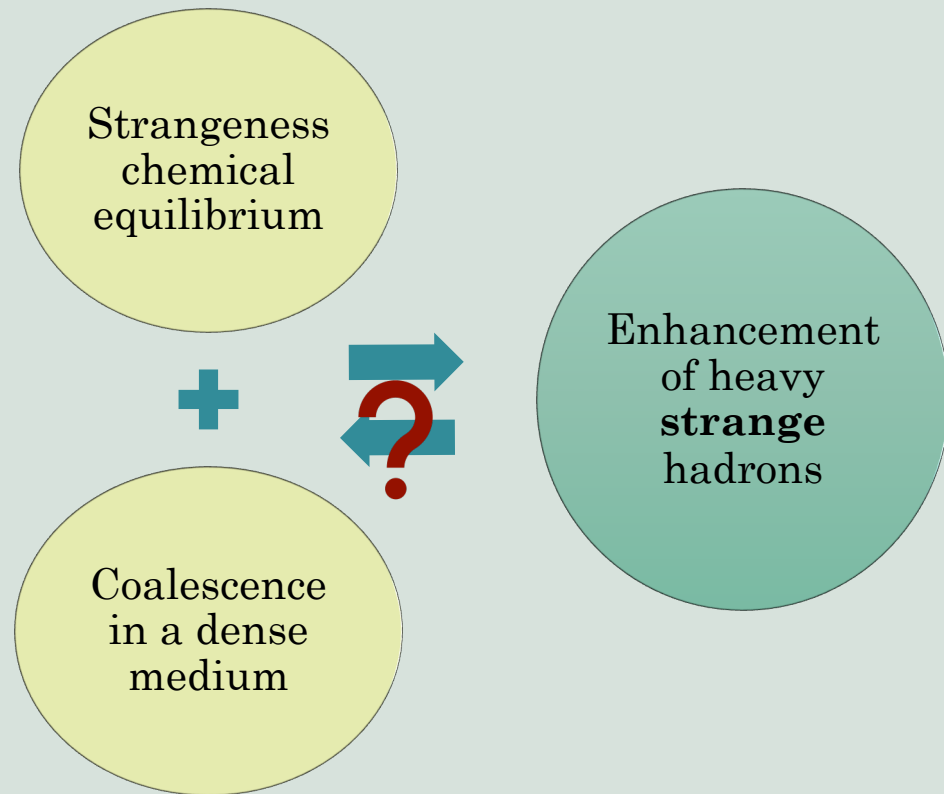
- The  $\Xi_c^+/\Lambda_c^+$  ratio is roughly constant as a function of  $p_T$  and shows the same behaviour in forward and backward collisions.
- No enhancement is shown when studying the dependence with  $N_{\text{clusters}}$ .



VELO clusters

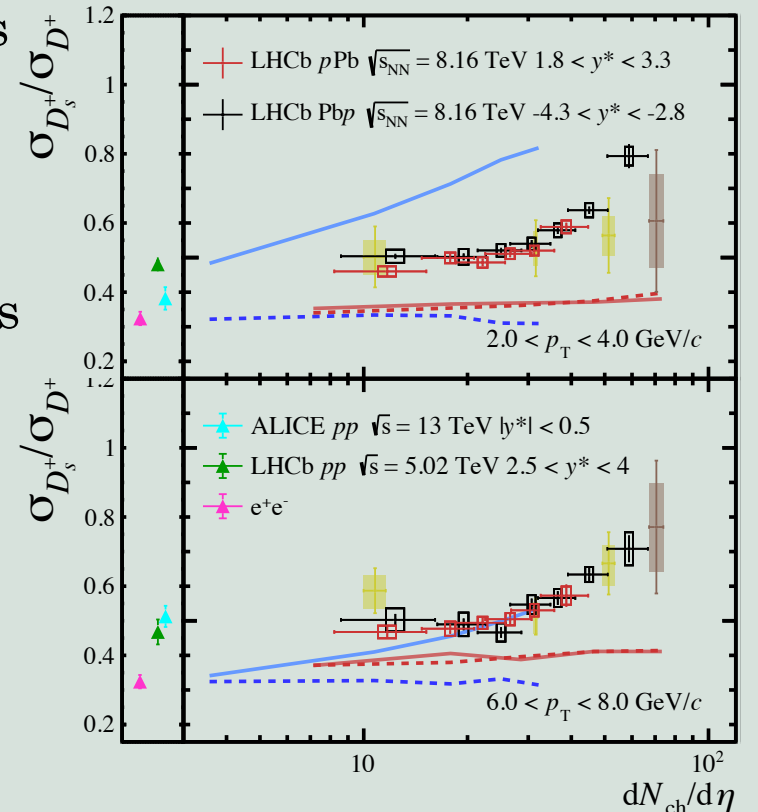
# Prospects

- Unifying multiplicity proxies among analyses may shed light over the interpretation of the results.
- Decorrelating the results from the multiplicity estimator to rule out local effects in charged particle multiplicity.
- Account for  $D^{*0/+} \rightarrow D^{0/+} + X$  contribution to  $D_s^+ / D^{+/0}$  ratios.
- Study strangeness in the light flavour sector.



# Conclusions

- The relative production of several strange to non-strange hadrons was studied in small collision systems at the LHCb.
- In  $pp$  collisions at  $\sqrt{s} = 13$  TeV, there is an observed enhancement of the  $B_s^0/B^0$  ratio at high multiplicity and low  $p_T$ . This enhancement is not observed when using backward tracks as multiplicity estimator.
- In  $pPb$  collisions at  $\sqrt{s_{NN}} = 5$  TeV the  $D_s^+/D^{0/+}$  the ratios don't show a clear trend with  $p_T$  or  $y$ .
- In  $pPb$  collisions at  $\sqrt{s_{NN}} = 8$  TeV, a significant enhancement of the  $D_s^+/D^+$  ratio is observed in events with high multiplicity.  
However, the baryon ratio of  $\Xi_c^+/\Lambda_c^+$  appears to be constant when studied as a function of  $N_{\text{clusters}}^{\text{VELO}}$ .



arXiv:2311.08490 NEW!

# Supplementary material

# $B_s^0/B^0$ ratio with multiplicity Efficiency cancelation

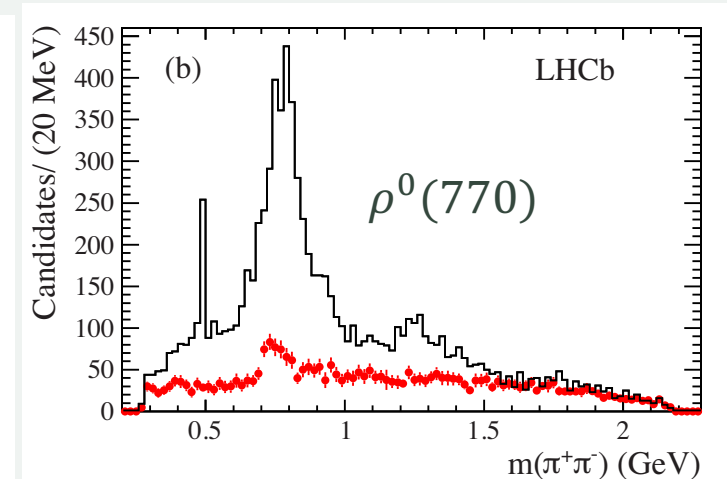
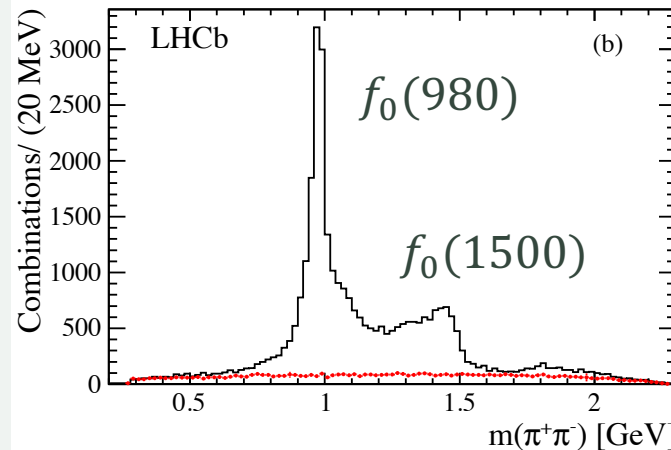


$$\frac{\sigma_{B_s^0}}{\sigma_{B^0}} = \frac{N_{B_s^0}}{N_{B^0}} \times \frac{\mathcal{B}_{B^0}}{\mathcal{B}_{B_s^0}} \times \frac{\varepsilon_{B_s^0}^{\text{acc}}}{\varepsilon_{B_s^0}^{\text{acc}}} \times \frac{\varepsilon_{B_s^0}^{\text{trig}}}{\varepsilon_{B_s^0}^{\text{trig}}} \times \frac{\varepsilon_{B_s^0}^{\text{PID}}}{\varepsilon_{B_s^0}^{\text{PID}}} \times \frac{\varepsilon_{B_s^0}^{\text{reco}}}{\varepsilon_{B_s^0}^{\text{reco}}}$$

- $\frac{\varepsilon_{B_s^0}^{\text{acc}}}{\varepsilon_{B_s^0}^{\text{acc}}}, \frac{\varepsilon_{B_s^0}^{\text{trig}}}{\varepsilon_{B_s^0}^{\text{trig}}}, \frac{\varepsilon_{B_s^0}^{\text{PID}}}{\varepsilon_{B_s^0}^{\text{PID}}} \sim 1$
- $\frac{\varepsilon_{B_s^0}^{\text{reco}}}{\varepsilon_{B_s^0}^{\text{reco}}} = 0.86 \pm 0.04$

Due to differences in the  $\pi^+\pi^-$  mass distribution

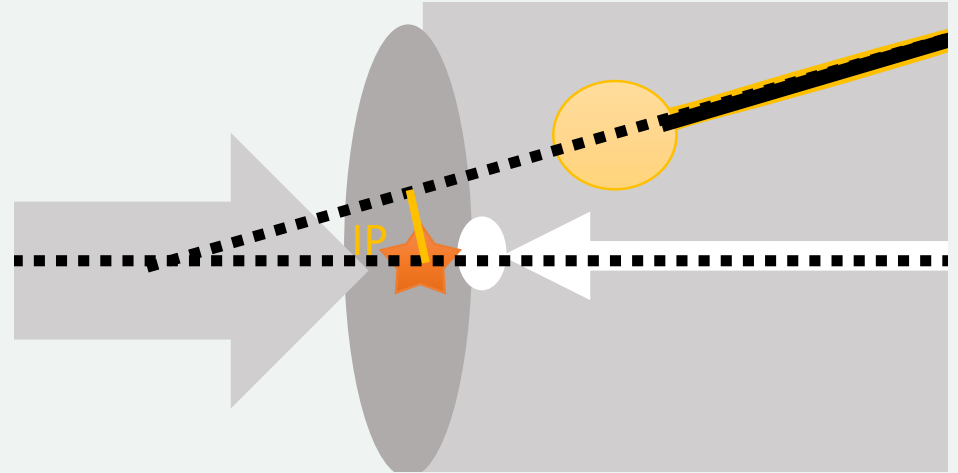
[Phys. Rev. D90 \(2014\) 012003](#)  
[Phys. Rev. D89 \(2014\) 092006](#)



# Prompt/non-prompt separation the $\log_{10}(\chi^2_{IP})$

$\chi^2_{IP}$  is the difference in the vertex-fit  $\chi^2$  of a given PV reconstructed with and without the candidate under consideration.

If the candidate is prompt, the  $\chi^2$  will improve when taking it into account.

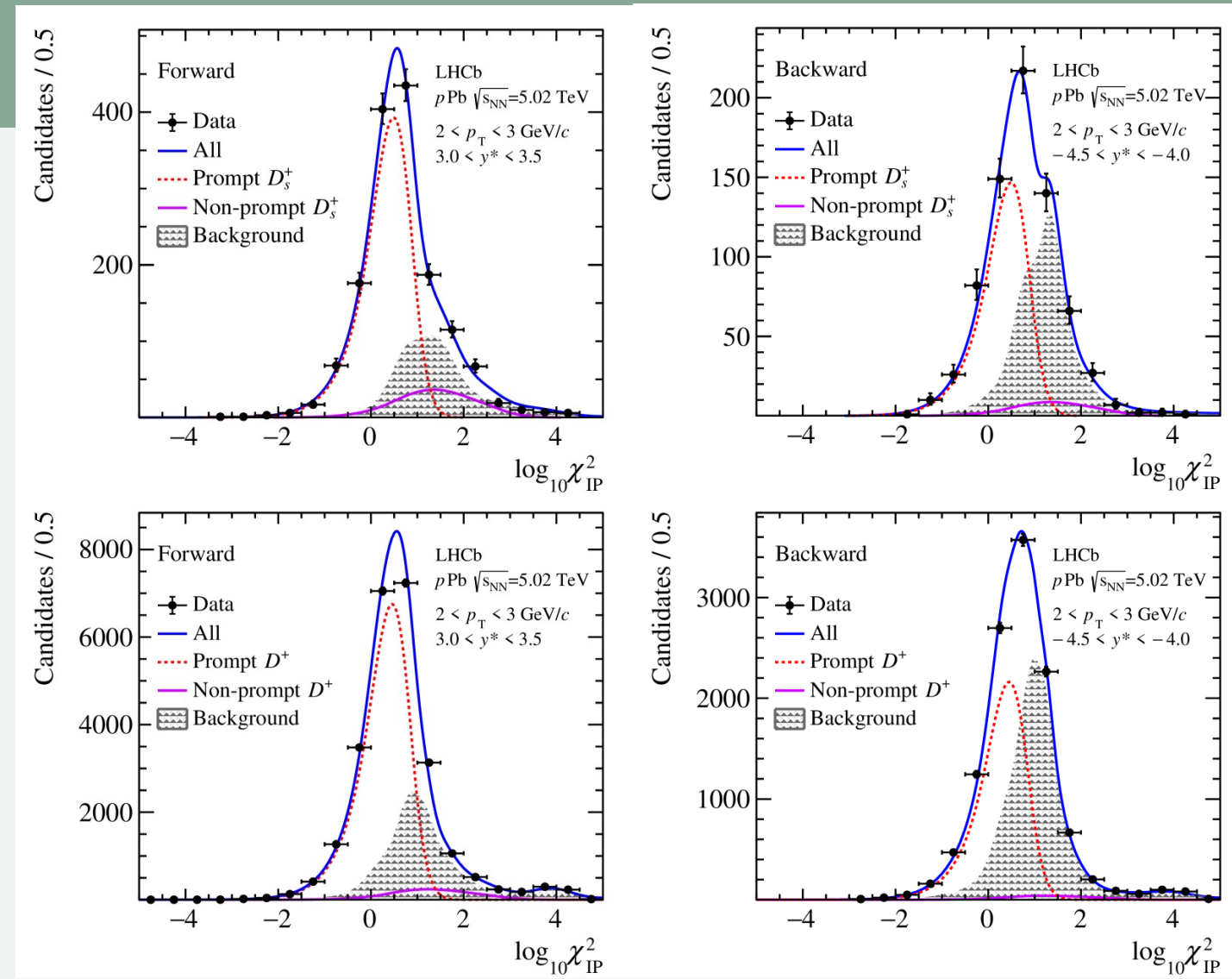


# Prompt/non-prompt separation

JHEP 01 (2024) 070

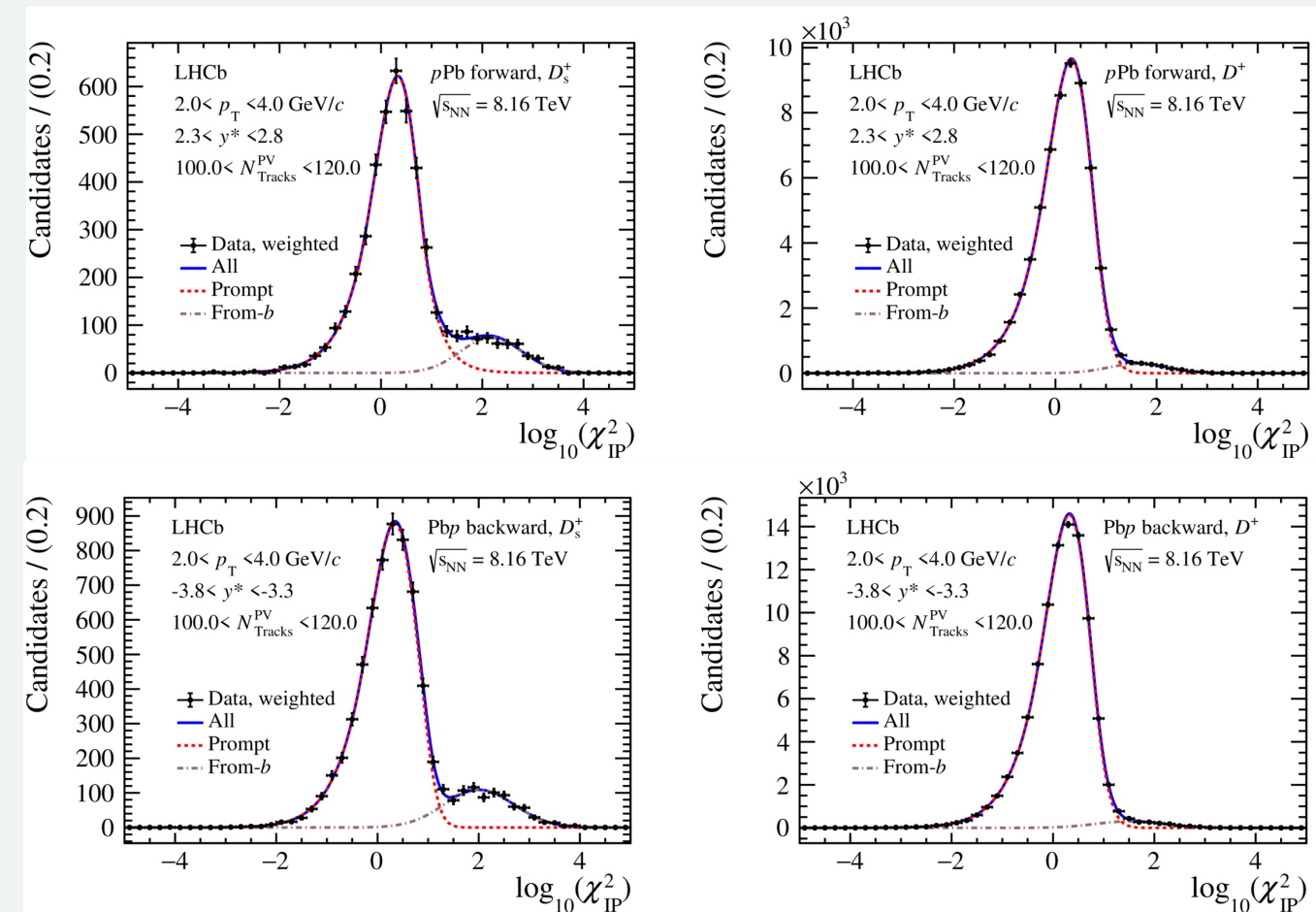
$D_s^+ / D^+ \text{ 5TeV}$

- In this case, a simultaneous fit to the mass and to the  $\log_{10}(\chi_{IP}^2)$  is performed.
- The shapes for the (non-) prompt contributions are determined from simulation, modelled with an asymmetric Bulkin curve with tails described by Gaussian functions.
- Width, asymmetry, tail coefficients and peak position of the non-prompt contribution are fixed to MC.
- The background of the  $\log_{10}(\chi_{IP}^2)$  is fitted by a kernel density estimate function



# Prompt/non-prompt separation

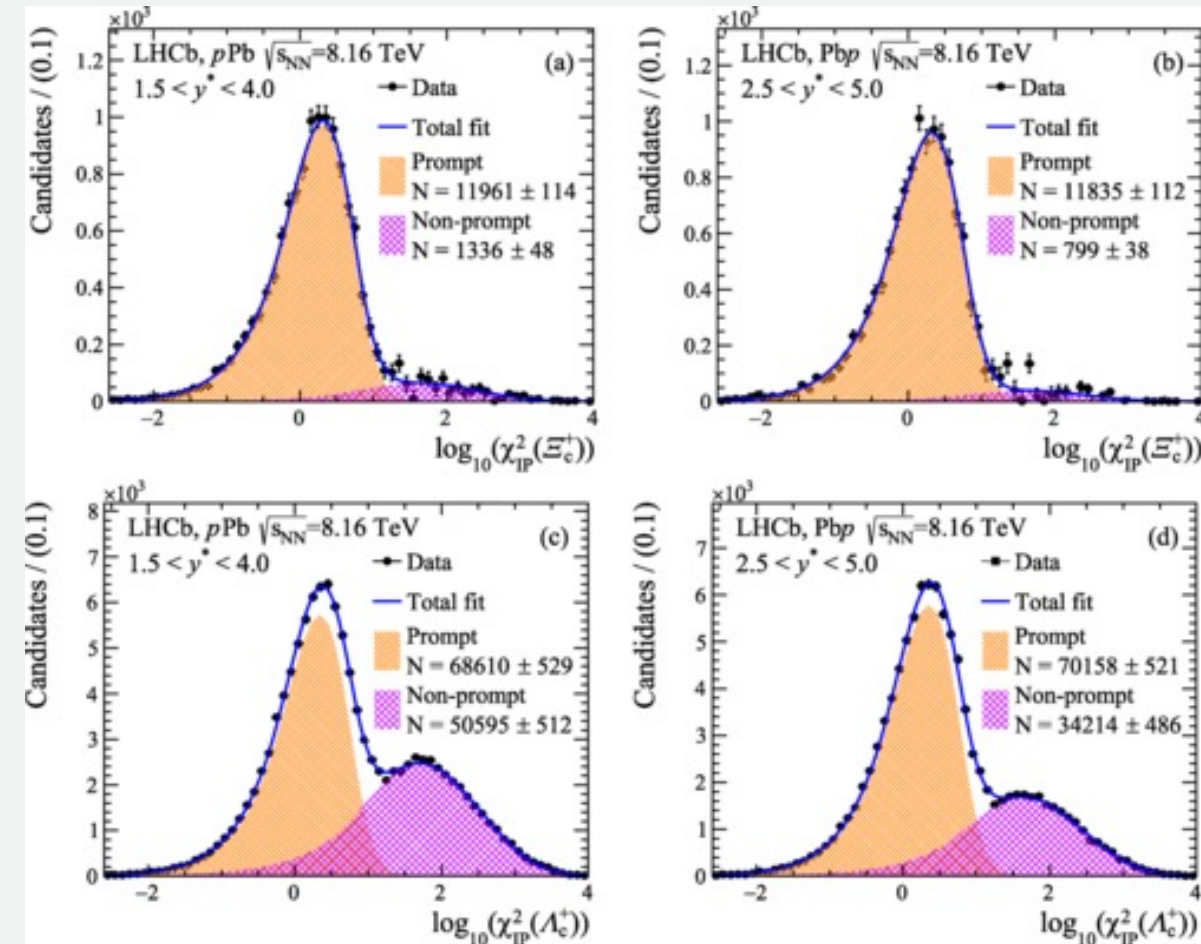
- After background-subtracting the data, a fit to the  $\log_{10}(\chi^2_{IP})$  is performed.
- The Bukin function is used to fit each contribution.
- The parameters of the function describing the non-prompt component are fixed from simulation, and the parameters from the prompt component are allowed to float.



# Prompt/non-prompt separation

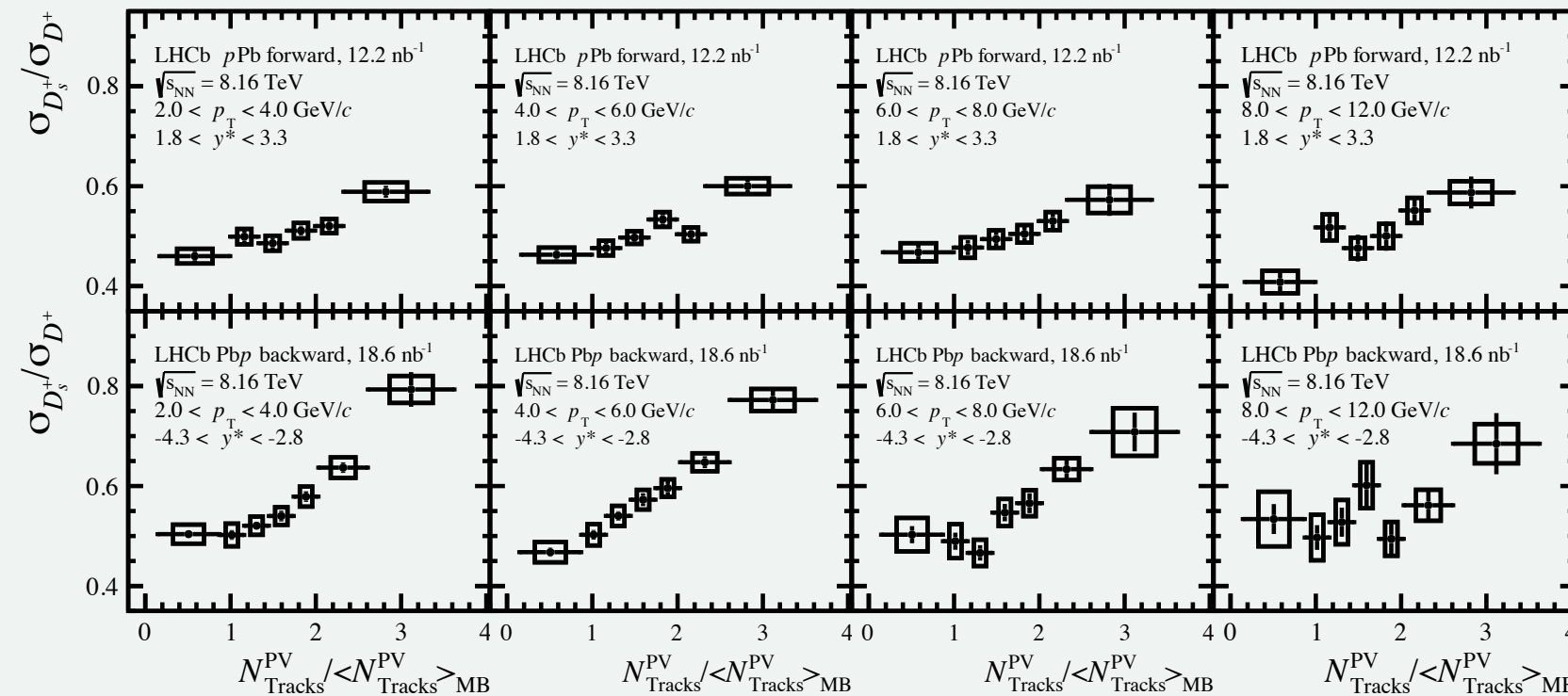
$\Xi_c^+/\Lambda_c^+$

- After background-subtracting the data, a fit to the  $\log_{10}(\chi^2_{IP})$  is performed.
- The Bukin function is used to fit each contribution with the asymmetry parameters taken from MC and letting the mean and variance to vary.



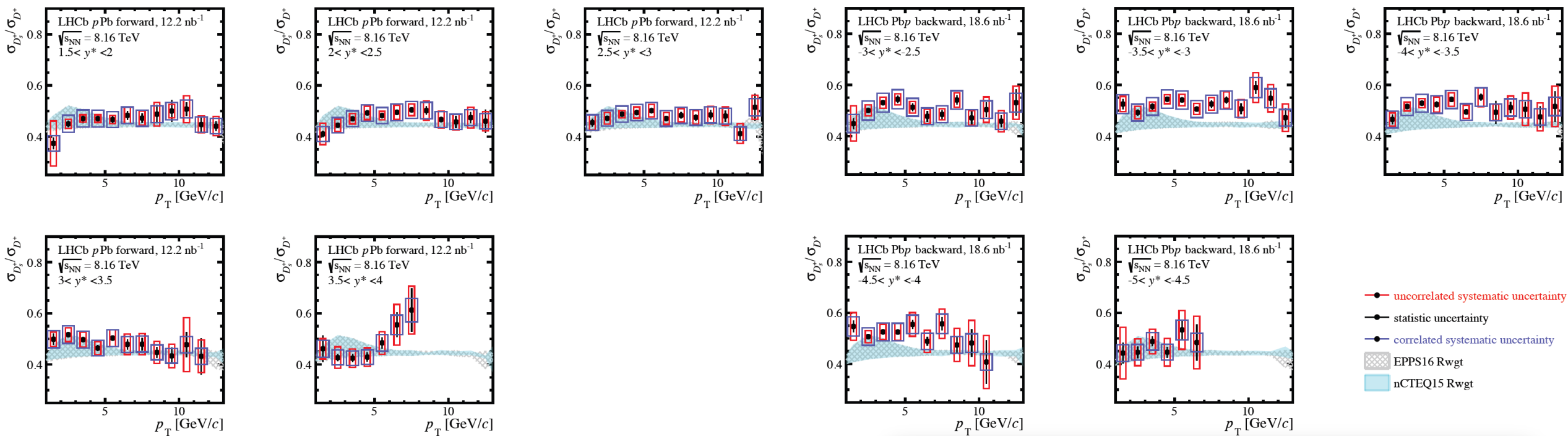
# $D_s^+ / D^+$ ratio

$p\text{Pb}$  collisions at  $\sqrt{s_{NN}} = 8 \text{ TeV}$



# $D_s^+ / D^+$ ratio

$p\text{Pb}$  collisions at  $\sqrt{s_{NN}} = 8 \text{ TeV}$



# $\Xi_c^+ / D^0$ ratio $p\text{Pb}$ collisions at $\sqrt{s_{NN}} = 8 \text{ TeV}$



The results are systematically below ALICE's, but they are compatible within uncertainties.

